

Aus dem Bereich Med. Biophysik
Theoretische Medizin und Biowissenschaften
der Medizinischen Fakultät
der Universität des Saarlandes, Homburg/Saar

**Vti1b-dependent interaction between lytic granules and
recycling TCR compartments is required for efficient function
of cytotoxic T lymphocytes**

*Dissertation zur Erlangung des Grades eines Doktors der
Naturwissenschaften*

der Medizinischen Fakultät
der UNIVERSITÄT DES SAARLANDES

2009

vorgelegt von: Bin Qu
geb.am: 27.03.1980 in Hebei, China

Tag des Promotionskolloquiums: _____

Dekan: _____

Vorsitzender: _____

Berichterstatter: _____

謹以此文献给我亲爱的父母

To my beloved parents

Index

1. Abstract	1
1. Zusammenfassung	3
2. Introduction	5
2.1 Immune system: a sophisticated orchestra	5
2.2 Cytotoxic T lymphocytes: all roads lead to death	7
2.3 Lytic granules: lethal kisses.....	9
2.3.1 Perforin	9
2.3.2 Granzymes	10
2.3.3 Cooperation between perforin and granzymes	11
2.3.4 Why CTLs remain intact after the lethal kiss delivery	12
2.4 The immunological synapse: face to face.....	13
2.4.1 T cell receptors	13
2.4.2 Immunological synapse formation	14
2.5 SNARE proteins: coordinators of intracellular trafficking	16
2.6 Disorders of human immunity: when killers cannot kill	18
2.7 Goals.....	21
3. Materials and methods	23
3.1 Reagents	23
3.2 Cells.....	23
3.2.1 PBL isolation	23
3.2.2 CD8 ⁺ T cell isolation	25
3.2.3 Cell culture	25
3.3 Electroporation of CD8 ⁺ T cells	26
3.4 Construction of cDNA.....	27

Index

3.5	Labeling recycling TCR in live cells.....	27
3.6	Immunofluorescence	27
3.7	Confocal microscopy.....	29
3.8	Epifluorescence deconvolution microscopy and time-lapse imaging	29
3.9	Evanescent-wave imaging.....	30
3.10	Lytic granule accumulation analysis	30
3.11	Small interfering RNA (siRNA).....	31
3.12	RealTime-PCR	31
3.13	Western blotting	33
3.14	Cytotoxicity assay	33
3.15	Data analysis.....	35
4.	Results.....	36
4.1	LG were tethered with rTCR.....	36
4.1.1	Recycling TCR was not in the position to trigger downstream signaling.....	36
4.1.2	Lytic granules were localized next to recycling TCR	38
4.1.3	Paired lytic granules are preferentially accumulated at the IS	42
4.2	Lytic granules are accumulated at the IS by tethering with rTCR	43
4.2.1	Paired lytic granules have longer dwell time at the IS	43
4.2.2	Paired lytic granules were secreted preferentially over single lytic granules...46	
4.2.3	The Golgi apparatus is involved in LG/rTCR pairing and plays a key role in LG/rTCR transport to the IS.....	48
4.3	Vti1b co-localized with paired LG and enhances the possibility for vesicle pairing	51

4.3.1	Analyzing the co-localization of SNARE proteins with lytic granules and recycling TCR	51
4.3.2	Vti1b co-localizes with paired lytic granules	54
4.3.3	The possibility of vesicle pairing was enhanced by Vti1b	55
4.4	Vti1b-dependent tethering of lytic granules and recycling TCR is required for CTL cytotoxicity	56
4.4.1	Vti1b is required for tethering of lytic granules and recycling TCR.....	56
4.4.1.1	Vti1b expression was down-regulated efficiently by siRNA	56
4.4.1.2	Down-regulation of Vti1b reduced the pairing rate.....	57
4.4.2	CTL cytotoxicity is impaired by down-regulation of Vti1b.....	59
4.4.2.1	Accumulation of lytic granules at the IS is impaired by down-regulation of Vti1b	59
4.4.2.2	CTL-mediated target cell killing is impaired by down-regulation of Vti1b	61
4.5	Vti1b may co-operate with AP-3 to mediate tethering	61
4.6	Model for paired vesicle transport	63
5.	Discussion	67
5.1	Significance of tethering of two organelles.....	67
5.1.1	<i>En passant</i> killing	67
5.1.2	Balance between TCR function and TCR down-modulation.....	69
5.1.3	General signaling mechanism.....	70
5.2	How Vti1b mediates tethering	71
5.3	What does the model tell us	72
5.4	Why the Golgi apparatus is reoriented to the IS.....	73

Index

5.5	Error estimation	74
5.5.1	The fate of tethered recycling TCR compartments	74
5.5.2	Two compartments or two sub-compartments	75
5.5.3	Secretory domain vs. multifocal IS in human CTLs	76
6.	References	77
7.	Publications	99
8.	Acknowledgements	100
9.	Curriculum Vitae	101

1. Abstract

Lytic granule (LG)-mediated apoptosis is the main mechanism by which cytotoxic T lymphocytes (CTLs) kill virus-infected and tumorigenic target cells. CTLs form a tight junction with the target cells called immunological synapse (IS). T cell receptors (TCR) are then quickly enriched at the IS. Lytic granules are also transported to the IS where they release their cytolytic contents inducing target apoptosis. To avoid unwanted killing of neighboring cells, exocytosis of lytic granules is tightly controlled and restricted to the IS. During my thesis work, I discovered the interaction of lytic granules with recycling TCR compartments (rTCR). This interaction is important for the accumulation and release of lytic granules at the IS as well as for CTL-mediated cytotoxic function. Lytic granules pair/tether with recycling TCR compartments in resting and conjugated CTLs. After target cell recognition, the paired lytic granules and recycling TCR compartments are co-transported to the IS, where recycling TCR compartments are required for the docking and release of lytic granules.

To search for the molecular mechanism of pairing, we screened SNARE proteins. We found that LG/rTCR pairs colocalize with the Qb-SNARE protein Vti1b. Down regulation of Vti1b by the RNA interference reduces the interaction of lytic granules and recycling TCR compartments. Consequently, accumulation of lytic granules at the IS and CTL-mediated cytotoxicity are also impaired in Vti1b-downregulated CTLs. Our data establish that the Vti1b-dependent interaction between lytic granules and recycling TCR compartments is required for CTL-mediated target cell killing.

To better understand the function of LG/rTCR pairing, a compartment model was formulated in co-operation with Prof. Heiko Rieger (Theoretical Physics, Saarbrücken),

based on the results from confocal microscopy experiments. The data showed that the rate of paired LG leaving the IS is much lower than the rate of paired LG approaching the IS, resulting in the accumulation of paired LG at the IS. In contrast, there is not much difference between the back and forward rate of single lytic granules. In addition, we determined for the first time the generation of new lytic granules *in vivo* after target cell recognition.

In summary, our data establish the tethering/pairing of LG and eTCR as a mechanism of rapid and efficient CTL-mediated target cell killing. The Qb-SNARE protein Vti1b is necessary for the interaction between LG and eTCR. This close interaction between LG and eTCR is required for the accumulation and secretion of LG at the IS. Vti1b down regulation by RNA interference decreased the probability of the interaction between LG and eTCR. As a result, LG accumulation and release at the IS were impaired and CTL-mediated cytotoxicity was reduced. This pairing mechanism sheds new light on understanding strictly controlled reorientation of lytic granules and CTL-mediated cytotoxicity.

1. Zusammenfassung

Zytotoxischen T-Lymphozyten (ZTL) töten Tumor- oder virusinfizierte Zellen hauptsächlich durch Apoptose, die durch die Inhaltsstoffe lytischer Granula (LG) vermittelt wird. Dabei bilden sie einen engen Kontakt mit ihren Zielzellen aus, die sogenannte Immunologische Synapse (IS), die unter anderem durch die Anreicherung von T-Zellrezeptoren (TZR) charakterisiert ist. Die LG werden zur IS transportiert, wo sie fusionieren und die Apoptose durch die Entleerung ihrer zytotoxischen Inhaltsstoffe in der Zielzelle auslösen. Um eine unerwünschte Abtötung benachbarter Zellen zu verhindern, muss die Exozytose der LG streng reguliert werden und darf nur an der IS stattfinden. Ich habe herausgefunden, dass LG mit intrazellulären Kompartimenten, die endozytierte T-Zellrezeptoren (eTZR) enthalten, interagieren. Diese Interaktion (oder auch Paarung zwischen den verschiedenen Organellen) ist unerlässlich für die Anreicherung und die Freisetzung der LG an der IS und damit für die Zytotoxizität der ZTL. Die LG können sowohl in ruhenden als auch in aktivierten ZTL mit den eTZR interagieren. Nach dem Kontakt mit einer Zielzelle werden die gepaarten LG/eTCR Kompartimente zusammen zur IS transportiert, wobei die eTZR Kompartimente notwendig für die Akkumulation und die Freisetzung der LG sind.

Um den molekularen Mechanismus der Interaktion besser zu verstehen, haben wir die Expression und Lokalisation vieler SNARE Proteine untersucht. Wir haben herausgefunden, dass LG/eTZR Kompartimente mit dem Qb-SNARE Protein Vti1b kolokalisieren. Eine Herunterregulation der Vti1b-Expression mittels siRNA-Technologie führt zu einer Reduktion der Anzahl der gepaarten LG/eTZR Kompartimente. Im Folgenden wird auch die Akkumulation der LG an der IS reduziert und dadurch die Zytotoxizität der ZTL erniedrigt. Diese Daten belegen, dass die Vti1b-abhängige

Interaktion zwischen LG und eTZR Kompartimenten für die Induktion der Apoptose in den Zielzellen notwendig ist.

Um die Funktion der LG/eTZR Kompartimente genauer zu analysieren, haben wir in Zusammenarbeit mit Prof. Heiko Rieger (Theoretische Physik, Saarbrücken), basierend auf unseren Konfokalmikroskopiedaten, ein sogenanntes Kompartimente-Modell entwickelt. Das Modell sagt unter anderem voraus, dass mit eTZR gepaarte LG eine geringere Wahrscheinlichkeit haben, von der IS wieder ins Zytosol zurücktransportiert zu werden als ungepaarte LG. Ebenfalls konnte mit Hilfe dieses Modells erstmalig *in vivo* die Neubildungsrate von LG nach Kontakt mit einer Zielzelle bestimmt werden.

Zusammenfassend kann man festhalten, dass die Interaktion/Pairung zwischen LG und eTZR Kompartimenten einen neuartigen Mechanismus darstellt, um eine schnelle und effiziente Abtötung von Zielzellen durch ZTL zu ermöglichen. Dabei ist das Qb-SNARE Protein Vti1b notwendig für die Interaktion zwischen LG und eTZR Kompartimenten. Die enge Interaktion zwischen LG und eTZR Kompartimenten ist entscheidend für die Anreicherung und Freisetzung von LG an der IS. Die Herunterregulierung der Vti1b-Expression mittels RNA-Interferenz erniedrigt die Wahrscheinlichkeit einer Interaktion zwischen LG und eTZR Kompartimenten. Nachfolgend wird die Akkumulation von LG an der Synapse inhibiert und dadurch die Zytotoxizität der ZTL reduziert. Der Interaktionsmechanismus zwischen LG und eTZR liefert ein besseres molekulares Verständnis dafür, wie LG streng kontrolliert an der IS lokalisieren, und damit ein besseres Verständnis für die ZTL vermittelte, LG-abhängige Zytotoxizität.

2. Introduction

2.1 Immune system: a sophisticated orchestra

The environment we are living in is filled with many potential pathogenic microorganisms. To fight against invaders, we have the immune system, which comprises a variety of cell types and proteins, working constantly regardless of the circumstances. A host defense system was already present in protozoans 2.5 billion years ago. New antipathogen devices have been constantly evolved in eukaryotes. In return, microorganisms also continually evolve new ways to evade host defense tactics. With this so-called host-versus-pathogen arms race, the most complicated and efficient immune system has been evolved in mammals¹⁻².

Picture what happens when a five-year-old girl gets her finger pricked with a rose thorn while playing in the garden. Within minutes or immediately after bleeding stops, the immune system sets off to eliminate the undesirable microbes introduced into the wound. The first response is executed by the innate immune system. The cells that belong to the innate immune system are already active even before invaders appear. Innate immunity depends on germline-encoded receptors that have evolved to recognize highly conserved pathogen-associated molecular patterns. Therefore the innate immune system is functioning in a generic, non-specific manner³⁻⁴. Innate immunity sometimes suffices to destroy invading microbes. If it does not, the girl relies on another system: acquired immune system.

The cells of the acquired immune system are specialized white blood cells, called lymphocytes. Patrolling the blood and lymph nodes, lymphocytes are normally at quiescent. But when they recognize foreign non-self antigens via the receptors on the plasma

2. Introduction

membrane, they become activated and start to proliferate. Lymphocytes can be divided into two major classes, B cells and T cells, which are both derived from hematopoietic stem cells in the bone marrow. B cells produce and secrete antibodies, which then bind to antigens to neutralize them or mark them for elimination. The human body contains more than 100 billion B lymphocytes, each lineage of B cell expresses a different antibody, so the complete set of B cell antigen receptors represent all the antibodies that the body produces ⁵⁻⁶.

T cells serve a variety of purposes: they recognize and kill cells bearing non-self molecules on their surface and they also help B lymphocytes produce antibodies. T cells only recognize the “non-self” antigens that have been processed and presented in combination with a major histocompatibility complex (MHC) molecule. There are two major subtypes of T cells: helper T cells and killer T cells. The helper T cells only recognize antigens bound to class II MHC molecules, while the killer T cell only recognize antigens bound to class I MHC molecules ⁷.

Helper T cells regulate both the innate and adaptive immune responses and help determine which types of immune responses the body will make to a particular pathogen. These cells have no cytotoxic or phagocytic activity and do not kill infected cells or clear pathogens directly. They instead control the immune response by directing other cells to perform these tasks. They are essential for determining B cell antibody class switching, for the activation and growth of killer T cells, and for maximizing bactericidal activity of phagocytes such as macrophages ⁷⁻⁸.

Killer T cells are also known as cytotoxic T lymphocytes (CTLs). Normally CTLs have CD8 molecules on the plasma membrane. They can eliminate pathogen-infected somatic cells and tumorigenic cells by destruction of target cells. Before killer T cells encounter the

corresponding antigen-presented target cells they are naive T cells and not yet killing competent. Once killer T cells recognize the target cells, they form a stable contact with the target cells. T cell receptors (TCR) are then activated to trigger downstream signaling pathways. It takes a few days for naive T cells to become killing competent effector killer T cells – CTLs ^{7,9-10}. The main focus of this study is on CTL-mediated cytotoxicity, in particular the precisely controlled release of cytotoxic granules.

2.2 Cytotoxic T lymphocytes: all roads lead to death

Both, the innate immune system and the adaptive immune system have their own killer cells: nature killer cells (NK cells) and cytotoxic T lymphocytes (CTLs) ¹¹. As a part of innate immune system, NK cells are constantly active, eliminating target cells in an antigen-unspecific manner. In contrast, each CTL lineage has unique T cell receptors (TCR), which are activated only by certain antigens ¹¹.

Before CTLs encounter the corresponding antigens, they patrol the peripheral blood system and lymphoid system ¹². In the lymph nodes, they examine all the accessible professional antigen-presenting cells, such as dendritic cells, macrophages and B cells ¹³. The professional antigen-presenting cells are responsible for processing the antigens from the non-self invaders and presenting these antigens (or parts of them) on their MHC molecules. Once antigens bound to the class I MHC molecules are recognized by matching TCR, the corresponding naive CTLs will be activated and begin the proliferation and maturation process ¹⁴⁻¹⁵. It takes 5-8 days for the activated CTLs to become fully mature and killing competent¹¹. During this period, helper T cells secrete certain cytokines to facilitate CTL proliferation and maturation ⁷.

2. Introduction

There are three known pathways in CTLs to destroy target cells. First and foremost, is the granule-mediated cytotoxicity¹⁶⁻¹⁷. Usually lysosomes function as protein degradation organelles, but lysosomes in CTLs are further specialized to work as secretory lytic granules for secretion¹⁸. The secretory lytic granules, also known as cytotoxic granules, are loaded with various cytotoxic proteins, such as the pore-forming protein perforin and the serine proteases called granzymes¹⁸. When CTLs encounter target cells, these secretory lytic granules are quickly reoriented towards the interface of CTLs and target cells¹⁹. Calcium (or Ca^{2+}) influx triggers the secretion of lytic granule to the tightly sealed cleft between the CTLs and their target cells²⁰. Cytotoxic proteins then enter target cells and cleave the substrate proteins, mostly caspases, to induce the apoptosis of target cells²¹.

The second pathway involved in target cell elimination is the Fas (CD95, a member of the tumour-necrosis factor receptor family of death receptors) pathway which requires neither calcium influx nor perforin²²⁻²³. The Fas molecule has a 'death' domain in its cytoplasmic tail. The engagement of the extra-cellular domain of the Fas monomer by Fas ligand on target cells results in the formation of a Fas trimer and activation of the cytosolic death domain. Trimerization of Fas triggers the activation of caspase-dependent pathway and the apoptosis of target cells²⁴.

As a complement to these two death-inducing strategies, several cytokines are secreted by CTLs, such as tumor-necrosis factor (TNF) and interferon- γ (IFN- γ), which mediate cytotoxic actions on target cells in the vicinity²⁵⁻²⁶.

Among these three strategies, granule-mediated cytotoxicity is the most important and most commonly used pathway in CTLs to destroy target cells. The other two pathways are maintained as backups. Only when the granule-mediated cytotoxicity pathway is compromised, do the other two pathways have a significant impact on the destruction of

target cells ²¹. Therefore, in this study we focus particularly on granule-mediated cytotoxicity.

2.3 Lytic granules: lethal kisses

To efficiently eliminate pathogen-infected or tumorigenic cells, dozens of cytotoxic proteins are loaded into secretory lytic granules. These cytotoxic proteins mainly belong to two major classes: membrane perturbing proteins and serine proteases.

2.3.1 *Perforin*

Perforin was first identified in 1985 and characterized as a calcium-dependent, pore-forming cytolytic protein ²⁷⁻²⁹. Perforin is comprised of a cleavable leader peptide that directs perforin into the secretory lysosomes, and a positively charged N-terminal sequence ³⁰. The calcium-dependent CD2 domain, which is essential for membrane binding of perforin, is located at the C-terminus ³¹. The final 20 amino acids of perforin contain an N-glycosylation site and a putative cleavage site, which are thought to be important for perforin activation ³².

Unlike the prosperous family of granzymes, perforin has no known isoforms. In fact, perforin has shown very little amino acid similarity to any other known proteins ³³. Such uniqueness suggests that perforin has some very essential non-redundant biological properties. Extensive studies using perforin knockout mice have revealed that perforin is required to maintain immune homeostasis and immune surveillance ³⁴⁻³⁸. When perforin-deficient mice were challenged with external pathogens, they exhibit a lymphoproliferative disorder and failed to eliminate pathogen-infected and/or transformed cells, which finally leads to spontaneous lymphoma ^{37,39-42}. In humans, perforin has been found to be

associated with a life-threatening immune disorder — familial haemophagocytic lymphohistiocytosis (FHL) — which is characterized by uncontrolled T lymphocyte and macrophage activation with a severe hyperinflammatory phenotype⁴³⁻⁴⁴. Dozens of mutations in perforin were identified in FHL patients and were considered to be the primary cause of the disease in up to 60% of the cases³³.

2.3.2 Granzymes

Eleven granzymes in mice and five granzymes in humans have been found. Granzyme A and B are the most redundant granzymes in mice and humans and have received the most attention⁴⁵. Granzyme A is a tryptase that induces caspase-independent cell death, which is a distinct pathway from granzyme B-mediated cell apoptosis⁴⁶⁻⁴⁷. Although granzyme A was the first granzymes to be described, much less is known about it than about Granzyme B⁴⁸. Granzyme A has long been thought to activate a slow cell-death pathway, because the oligonucleosomal DNA fragments released from the cells transfected with granzyme A and perforin cannot be detected until 16 hours after treatment, a timescale that is similar to slow cell-death pathway initiated by ligating cell-surface death receptors⁴⁹⁻⁵⁰. However, later studies showed that the features of apoptosis — membrane blebbing, mitochondrial dysfunction and loss of plasma membrane integrity — appeared within minutes in cells treated with recombinant granzyme A and perforin⁵¹. One explanation of this discrepancy is that DNA is less damaged by granzyme A than by an equivalent amount of granzyme B, therefore the DNA fragments are too large to be released quickly from the nucleus into culture supernatants⁴⁵.

Unlike the other serine proteases, granzyme B cleaves after aspartic acid residues, like the caspases⁵²⁻⁵³. It activates caspase-mediated apoptosis by cleaving caspases, particularly the key executioner caspase-3⁵⁴⁻⁵⁵ or by directly cutting downstream caspase substrates⁵⁶⁻⁵⁸. The activation of the caspase cascade is not the only pathway used by granzyme B to induce target cell death. Even when the caspase activity is completely blocked, granzyme B-mediated cell apoptosis is fully functional⁵⁹⁻⁶¹. By cleaving BID (BH3-interacting domain death agonist), granzyme B can destroy the integrity of the mitochondrial outer membrane and thereby initiate the mitochondria-mediated apoptosis pathway⁶²⁻⁶⁵. Moreover, granzyme B can directly unleash the caspase-activated DNase (CAD) by directly cleaving its inhibitor ICAD^{59,66}.

2.3.3 Cooperation between perforin and granzymes

Perforin was thought to be able to induce target cell apoptosis itself by forming poly-perforin pores on the plasma membrane of target cells, which results in osmotic instability and loss of intracellular contents⁶⁷. However, the discovery of the pro-apoptotic activity of the granzymes altered this model. It is no debate that perforin is required for granzymes to execute their functions in target cells, because both CTLs and NK cells from perforin-deficient mice completely lose the ability to kill target cells³⁶. But how exactly perforin cooperates with granzymes is still an enigma. One model is that the transmembrane pores formed by perforin act as passive channels for granzymes to enter target cells, which has been challenged by the fact that granzymes can enter target cells by endocytosis independently of perforin⁶⁸⁻⁶⁹. Another model is that perforin is irrelevant to granzyme entry target cells but it facilitates granzymes to escape from the endocytosed compartments into the cytosol. This model receives support from the finding that, without perforin,

granzymes can still be endocytosed but cannot kill target cells⁷⁰⁻⁷¹. Similar to this model, another model was developed, which suggests that the mannose 6-phosphate receptor can function as a candidate surface receptor to mediate the endocytosis of granzymes, particularly granzyme B, by internalizing the serglycin-based granzyme-bound macromolecular complex⁷²⁻⁷³.

2.3.4 Why CTLs remain intact after the lethal kiss delivery

Perforin and granzymes exhibit potent abilities to destroy target cells both externally and internally. However, perforin and granzymes are completely innocuous to the host cells that synthesize, store and secrete them. How can such a duality be achieved? How could killer cells protect themselves from lethal hits of cytotoxic proteins?

The first essential step for perforin to form pores is to coordinate calcium ions with its C2 domain, which is required to bind to the phospholipids membrane⁷⁴⁻⁷⁵. In fact at least 200 μM of free calcium is required to maximize membrane binding capacity of perforin and thereby to achieve full cytolytic activity³¹. But in resting cells there is only 50-200 nM free calcium and moreover, even in activated degranulating killer cells the cytosol free calcium concentration never exceeds 2-5 μM ⁷⁶. The physiological intracellular calcium concentration makes it impossible for perforin to bind calcium, which is the prerequisite for poly-perforin-pore formation. In addition, perforin has been shown to bind to the lipid bilayer only when the $\text{pH} > 6.2$ ³¹. Therefore the acidic environment of secretory lytic granules is a safeguard to restrain the cytolytic activity of perforin.

Another way CTLs protect themselves is by expressing granzyme-specific inhibitors, members of the serpin (serine proteinase inhibitor) superfamily⁷⁷. For example, the

intracellular inhibitor of human granzyme B, proteinase inhibitor-9 (PI-9), is expressed in lymphocytes⁷⁷⁻⁷⁸ and is up-regulated by modulators of inflammation like lipopolysaccharide, IFN- γ and IL-1 β ⁷⁹⁻⁸⁰. In case some granzymes inadvertently re-enter CTLs, serpins can inactivate their targets either by covalently and irreversibly binding to the active site of the enzyme or by forming noncovalent complexes⁸¹⁻⁸².

A lysosomal protein, cathepsin B, which remains at the outer plasma membrane after granule release, can also protect CTLs from self-destruction by cleaving perforin following its release into the synaptic cleft⁸³. Moreover, the lytic granules contain the Ca²⁺-binding protein and chaperone calreticulin, which binds to perforin and potently inhibits perforin-mediated damage⁸⁴⁻⁸⁵. Calreticulin might protect lytic granules from autolysis by perforin polymerization, but whether it plays also an inhibitory role after granule exocytosis is still unclear⁴⁵.

2.4 The immunological synapse: face to face

2.4.1 T cell receptors

Successful elimination of ‘non-self’ invaders or ‘altered-self’ somatic cells by CTLs requires that antigens presented on those cells must be recognized by cognate T cell receptors (TCR). TCR activation induces downstream signaling and an effective cytotoxic response. TCR initiates a plethora of pathways, thereby regulating diverse cellular functions such as proliferation, differentiation and apoptosis⁸⁶. The TCR polypeptides themselves have very short cytoplasmic tails, and all proximal signaling events are mediated through the CD3 molecules, which comprises γ , δ , ϵ and the disulfide linked ζ - ζ chains⁸⁷.

The TCR/CD3 complex plays a pivotal role in mediating cell recognition events. TCR engagement by antigens triggers the tyrosine phosphorylation of so-called ITAMs (immuno-receptor tyrosine-based activation motif), which are present in the TCR-associated CD3 complexes⁸⁸⁻⁹⁰. ITAMs function by orchestrating the sequential activation of the Src-related PTKs, Lck and Fyn⁹¹⁻⁹², which initiate TCR signaling, followed by ZAP70, which further amplifies the response⁹³⁻⁹⁵. Various proteins are then phosphorylated, including the transmembrane adaptors LAT (Linker Activator for T-Cells) and cytoplasmic adaptor SLP-76 (SH2-domain-containing leukocyte protein of 76kDa)⁹⁶⁻⁹⁷. Protein tyrosine phosphorylation subsequently leads to the activation of multiple pathways, including ERK (extracellular signal regulated kinase), JNK (c-Jun N-terminal kinase), NF-KappaB (nuclear factor-KappaB) and NFAT (nuclear factor of activated T-cells) pathways, which ultimately induce effector functions⁹⁸⁻¹⁰¹.

During the IS formation, TCR are quickly polarized and enriched at the IS. This enrichment of TCR is a necessary step to recruit effector molecules and initiate downstream signaling, which eventually leads to the apoptosis of target cells¹⁰²⁻¹⁰³. TCR recycling is essential for targeting TCR to the IS¹⁰⁴⁻¹⁰⁶. TCR are internalized and recycled back to the cell surface in both constitutive and antigen-dependent manner¹⁰⁷⁻¹¹⁰. When TCR recycling is blocked, the enrichment of TCR at the IS is drastically reduced¹⁰⁴⁻¹⁰⁶.

2.4.2 Immunological synapse formation

The word ‘synapse’ is derived from the Greek words, which means ‘junction’ or ‘connection’ between two similar entities. It is used commonly to describe neuronal connections. The ‘immunological synapse’ (IS) was termed by Michael Dustin to describe the interactions between T cells and their target cells¹¹¹. One prominent feature of the

immunological synapse is that the spatial segregation of several proteins patterns as a well-organized doughnut-like structure, termed supra-molecular activation complexes (SMACs). The center region of the SMAC (cSMAC) is enriched in TCR and one of its downstream effector molecules, protein kinase C- θ (PKC- θ)¹¹². Surrounding cSMAC is a peripheral ring, pSMAC, which is dominated by adhesion molecules — integrin leukocyte function-associated antigen 1 (LFA1) and cytoskeletal linker talin¹¹². The pSMAC is encircled by large and bulky molecules, CD43 and CD45, locating in a region distal to the synapse — dSMAC¹¹².

After target cell recognition, a drastic rearrangement takes place in T cells to establish the IS. Within minutes after T-cell recognition of a target cell, signals that emanate from the TCR lead to rapid cytoskeleton polarization, which involves F-actin polymerization¹¹³⁻¹¹⁴ and the reorientation of microtubule-organization center (MTOC) and Golgi apparatus towards the T cell-target cell interface¹¹⁵. TCR are also rapidly transported towards and enriched at the IS^{112,116}. Lytic granules, the cytotoxic protein carriers, are also relocated and accumulated at the IS¹⁹.

The T-cell cytoskeleton is composed of actin filaments, microtubules and intermediate filaments¹¹⁷. The T cell-target cell interaction leads to rapid F-actin polymerization in the form of a lamellipodium structure, which increases the interactive interface between the T cell and the target cell. The lamellipodium then contracts, leaving F-actin redistributed at the interface between the T cell and the target cell¹¹³⁻¹¹⁴. During IS formation, an actin-rich structure known as the distal-pole complex on the opposing side of the cell emerges¹¹⁸. Disruption of F-actin itself or the depletion of cytoskeletal regulators impairs IS formation and T-cell activation^{114,119-120}. In addition, CD3 ζ (also known as CD247) has been shown to associate with the T cell cytoskeleton¹²¹⁻¹²². Many studies have shown that numerous

TCR-activated signaling molecules are required for actin accumulation at the IS, including the TCR-proximal kinases *lck*, *ZAP70*¹²³, *ITK* (interleukin-2-inducible T-cell kinase)¹²⁴⁻¹²⁵, calcium signaling¹¹³ and the adaptors *LAT* and *SLP76*¹²⁶⁻¹²⁷. Moreover, deficiencies of key actin-regulatory proteins — for example, *WASP* (Wiskott-Aldrich syndrome protein), *VAV1* and *WIP* (*WASP*-interacting protein) — result in profound defects in lymphocyte activation and development¹²⁸⁻¹³⁰.

Similar to the actin rearrangement during IS formation, the MTOC (or centrosome) relocalization in T cells also requires many signaling molecules, including *Lck*, *FYN*, *ZAP70*, *LAT*, *SLP76*, *VAV1*, *CDC42* and intracellular calcium¹³¹⁻¹³⁵. MTOC reorientation appears to control the directed secretion of lytic granules, which might travel along microtubules in a minus-end-directed manner to the centrosome¹³⁶. Whether contact between the centrosome and the plasma membrane in CTLs is necessary for the delivery of lytic granules to the IS, as suggested by Sinchcombe *et al.*, has not been yet confirmed by other groups.

2.5 SNARE proteins: coordinators of intracellular trafficking

The SNARE (soluble-N-ethylmaleimide-sensitive-factor attachment protein receptor) protein family is known to be involved in intracellular vesicle budding, vesicular transport and vesicle fusion¹³⁷⁻¹³⁹. Until now, 38 members of the mammalian SNARE family have been reported (Table 1). Originally SNARE proteins were classified as v- (vesicle-associated) or t- (target-membrane) SNAREs, on the basis of their locations and functional roles in a typical vesicle-membrane fusion process. This terminology was challenged by the fact that it is not always clear which side is the vesicle or the cognate target membrane

2. Introduction

as fusion events often occur also between two vesicles. An alternative structure-based classification has now been suggested based on the following findings. Cognate SNARE proteins form a four-helix bundle complex, composing of 16 β -sheet layers. At the layer 0 there are four highly conserved residues — one arginine (R), three glutamine (Q) — contributed by the four SNARE motifs, respectively¹³⁸. On the basis of the central functional residue in their SNARE motif, the family is divided into R- (mostly corresponding to v-SNAREs) and Q-SNAREs (mostly corresponding to t-SNAREs). Q-SNARE proteins are further subclassified into Qa-, Qb-, Qc- and Qb,c-SNAREs, depending on the relative position of the conserved glutamine in the layer 0. Normally one SNARE protein contributes only one SNARE motif, whereas Qb,c-SNARE proteins contain two SNARE motifs. A functional four-helix bundle SNARE complexes require one R-SNARE and three Q-SNAREs to form R-Qa-Qb-Qc or R-Qa-Qb,c configurations¹³⁹⁻¹⁴⁰.

Q- and R-SNARE family members currently identified:

Qa. Syntaxin 1 (STX1), STX2, STX3, STX4, STX5, STX7, STX11, STX13, STX16, STX17 and STX18

Qb. GS27 (Golgi SNARE of 27 kDa), GS28, Vti1a (vesicle transport through interaction with the t-SNARE homologue 1a) and Vti1b

Qc. STX6, STX8 and STX10, GS15, BET1 and SLT1 (SNARE-like tail-anchored protein 1)

Qb,c. SNAP23, SNAP25, SNAP29 and SNAP47

R. VAMP1 (vesicle-associated membrane protein 1), VAMP2, VAMP3, VAMP4, VAMP5, VAMP7, VAMP8, ERS24 (SEC22b) and YKT6

Unclassified. D12, SEC20, SEC22a and SEC22c.

Table 1. Members of SNARE family¹⁴¹.

The functions of SNARE proteins in T cells are only beginning to be elucidated. Das *et al.* showed that the Q-SNARE proteins syntaxin 4 and SNAP23 are clustered at the IS of

Jurkat T cells, and inactivation of VAMP2 and VAMP3 with tetanus toxin notably reduced the delivery and enrichment of TCR at the IS¹⁰⁶. This indicates that SNARE proteins may play important roles at the immunological synapse and VAMP2 and/or VAMP3 are involved in TCR transport and enrichment at the IS.

Immune disorders induced by deficiencies of SNARE proteins and SNARE-regulatory proteins in humans and mouse models provide additional evidences of SNARE functions in CTLs. The lack of syntaxin 11 has been linked to the life-threatening familial hemophagocytic lymphohistiocytosis (FHL) type 4, in which CTLs and NK cells are incapable of releasing cytotoxic proteins from lytic granules to eliminate pathogen-infected cells¹⁴²⁻¹⁴⁴. This suggests that syntaxin 11 is essential for lytic granule exocytosis. In addition, mutations in the Munc13-4 or Rab27a gene, two SNARE-regulatory proteins, cause defects in lytic granule release, accounting for severe immune disorders¹⁴⁵⁻¹⁴⁶.

2.6 Disorders of human immunity: when killers cannot kill

Several naturally occurring mutants of the granule-dependent cytotoxicity pathway have been described in humans and mice. Their molecular basis has been recently identified, which provides new insights into our understanding of the lytic granule-mediated cytotoxicity process. All of these disorders listed in Table 2 result in a specific condition termed hemophagocytic syndrome, which is known as hemophagocytic lymphohistiocytosis (HLH) in humans¹⁴⁷. HLH is characterized by unremitting CD8+ T cell proliferation, activation and infiltration of visceral organs combined with macrophage activation (hemophagocytosis), and in the deleterious secretion of multiple cytokines including interferon- γ , interleukin 1 (IL-1), IL-6, IL-18 and tumour necrosis factor α ¹⁴⁸.

2. Introduction

Steps of lymphocyte cytotoxicity	Disease	Gene	Protein	Function
Cell activation	X-linked lymphoproliferative syndrome	<i>SH2DIA</i>	SAP	Adaptor
Polarization of lytic granules	Hermansky-Pudlak syndrome 2	<i>AP3B1</i>	AP3B1	Sorting
Tethering of lytic granules to plasma membrane	Griscelli syndrome 2	<i>Rab27a</i>	Rab27a	GTPase Granule movement
Priming for fusion of lytic granules	Familial hemophagocytic lymphohistiocytosis 3	<i>UNC13D</i>	Munc13-4	Priming
Exocytosis	Chediak-Higashi syndrome	<i>LYST</i>	LYST	Unknown
Fusion with plasma membrane	FHLH4	<i>Syntaxin-11</i>	Syntaxin-11	Fusion?
Killing	FHLH2	<i>PRF</i>	Perforin	Pore-forming protein

Table 2. Genetic diseases that cause the hemophagocytic syndrome (HLH) ¹⁴⁷.

The X-linked proliferative syndrome (XLP) is a complex disease caused by mutations of the *SH2DIA* gene, which encodes SLAM-associated protein (SAP), a 17 kd protein mostly expressed in T, natural killer (NK) and natural killer T (NKT) lymphocytes. Absence or dysfunction of SAP results in fulminant infectious mononucleosis (a severe form of HLH) in 60% of the cases upon encounter of the Epstein-Barr virus (EBV), to lymphomas in 20–30% of the cases, and to hypogammaglobulinemia in 30% of the cases, as well as to other less frequent manifestations ¹⁴⁹⁻¹⁵⁰.

The Hermansky Pudlak syndrome (HPS) is a group of genetic diseases, associated with partial albinism and bleeding disorders ¹⁵¹⁻¹⁵². Mutations in 7 genes in humans and 16 in mice have been documented to be involved in HPS ¹⁵³. HPS II is caused by mutations in the β subunit of the AP-3 (adaptor protein-3) ¹⁵⁴⁻¹⁵⁵. AP-3 is reported to be involved in sorting proteins from early endosomes to lysosomes ¹⁵⁶⁻¹⁵⁸. It has been shown that CTLs from HPS II patients fail to polarize lytic granules to the IS, whereas the MTOC polarizes normally ¹⁵⁴. It has thus been postulated that AP-3 is necessary for sorting a yet unidentified protein required for lytic granule motility ¹⁴⁷.

Griscelli syndrome (GS), a rare autosomal recessive disorder, results in pigmentary dilution of the skin and the hair, the presence of large clumps of pigment in hair shafts and an uncontrolled T-lymphocyte and macrophage activation syndrome (known as

2. Introduction

haemophagocytic syndrome, HS) ¹⁵⁹⁻¹⁶⁰. The CTLs, derived from GS patients as well as from the GS murine counterpart, ashén mice, display defective lytic granule-mediated cytotoxicity ^{146,161}. Biallelic mutations in the gene encoding Rab27a — a ubiquitously expressed small GTP-binding GTPase protein — are responsible for GS II and the ashén phenotype ^{146,161}. Rab27a-defective CTLs are unable to release lytic granules, although polarization is preserved. Using electron microscopy it has been shown that lytic granules can still accumulate at the IS, but fail to dock at the plasma membrane ¹⁴⁶. At present it is not known which interacting partner(s) is (are) involved in Rab27a-mediated lytic granule docking at the plasma membrane.

Familial hemophagocytosis lymphohistiocytosis (FHL) is characterized by an early onset HLH and defective cytolytic activity ¹⁶². Biallelic mutations of UNC13D encoding Munc13-4 were found in FHL type III patients. In Munc13-4 deficient CTLs lytic granules can polarize to the IS and dock at the plasma membrane, but fail to undergo exocytosis ¹⁴⁵. Munc13-4 is a member of the Munc13 family, which is crucial for Ca²⁺-triggered exocytosis at neuronal synapses ¹⁶³. It has been proposed that Munc13-4 mediates lytic granule fusion with the plasma membrane at the IS ¹⁴⁷.

In another variant of FHL (FHL4) observed in the Turkish and Kurdish population, a genetic deficiency in syntaxin-11 has been described ¹⁴⁴. Syntaxin 11 was found to be enriched in tissues of the immune system including thymus, spleen and lymph nodes ¹⁶⁴. It localizes in late endosomes, intermediate compartments and trans-golgi network ¹⁶⁴⁻¹⁶⁵. Although the precise functions of syntaxin-11 in lytic granule exocytosis are still obscure, it is certainly possible that syntaxin-11 is involved in SNARE-mediated fusion of lytic granules with plasma membrane.

Perforin deficiencies account for FHL2, which is responsible for 30–40% of all FHL conditions⁴⁴. Several different mutations have been characterized that lead to an absence or a defective cleavage of perforin, which is required for its function¹⁶⁶⁻¹⁶⁷. This result stresses the indispensable key role of perforin in lytic granule-mediated cell death.

2.7 Goals

As described above, TCR recycling is important for TCR enrichment at the IS and for many of the down stream signaling culminating in T cell activation. But most of the recycling TCR enriched at the IS are not incorporated into the plasma membrane, in other words, they are not at the position to trigger downstream signaling cascades. In addition, as lateral movement of TCR within the plasma membrane can also contribute to TCR enrichment at the IS, it is not necessary to relocate recycling TCR to the IS for maintaining down stream signaling. However, if TCR recycling is blocked, T-cell function is drastically impaired. If re-localization of recycling TCR to the IS is not for triggering or maintaining downstream signals, what exactly are the functions of recycling TCR at the IS? Secretion of lytic granules at the IS only is pivotal to restrain CTL-induced cell death to the desirable target cells, but not bystander cells. Stinchcombe *et al.* suggest that the MTOC is involved in delivery of lytic granules to the IS. Many studies in genetic mutations, which lead to severe immune disorders, also show hints of how lytic granule release at the IS is regulated. Yet the detailed mechanism of how lytic granules accumulate preferentially at the IS is not completely elucidated. Although TCR enrichment and lytic granule accumulation at the IS are two prominent features of IS maturation, no evidence has been ever shown that these events are linked in any way.

2. Introduction

Therefore the goals in this study are focused on:

1. What is the functional importance of TCR recycling to the IS in CTLs?
2. Are LG and TCR accumulation at the IS linked or independent of each other?
3. Is the MTOC translocation the only mechanism to control lytic granule accumulation at the IS?
4. Which SNARE protein(s) play(s) important role(s) in lytic granule accumulation and release at the IS?

3. Materials and methods

3.1 Reagents

All chemicals not specifically mentioned were from Sigma (highest grade). The reagents used in our experiments include: Alexa⁴⁸⁸-labeled anti-CD3 mAb (UCHT1, 300415, Biolegend), Alexa⁶⁴⁷-labeled anti-CD3 mAb (UCHT1, 300416, Biolegend), Alexa⁶⁴⁷-labeled anti-perforin mAb (dG9, 308110, Biolegend), FITC-labeled anti-perforin mAb (dG9, 21146093S, ImmunoTools), Alexa⁵⁶⁸ goat anti-rabbit secondary Ab (A-11031, Invitrogen) and Alexa⁵⁶⁸ goat anti-mouse secondary Ab (A-11011, Invitrogen), rabbit polyclonal Vti1b antibody (164002, Synaptic Systems), anti-Vti1b mAb (611405, BD Biosciences), anti-human Adaptin delta mAb (611328, BD Biosciences), Alexa⁴⁸⁸-labeled Transferrin (T13342, Invitrogen), anti- γ -tubulin (T5192, Sigma). For TIRF microscopy, the antibodies against human CD3 (BB11, Euroclone) and CD28 (555725, BD Bioscience) were used for coating the coverslips.

3.2 Cells

3.2.1 PBL isolation

Human peripheral blood lymphocytes (PBL) were obtained from healthy donors as described previously¹⁶⁸. Research carried out for this study with human material has been approved by the local ethics committee. The leucocyte reduction chambers (LRS chamber) were used for PBL isolation. The LRS chambers were kindly provided by the Blutspendedienst der Universitätskliniken des Saarlandes der Abteilung für klinische

3. Materials and methods

Hämostaseologie und Transfusionsmedizin. The information of the blood donors was obtained the next day after PBL preparation, including the gender, the age, the blood group, HIV and hepatitis positive or negative. The procedure of PBL isolation is as follows:

- Transfer 15-17 ml lymphocyte isolation buffer (LSM1077 Lymphocyte, J15-004, PAA Laboratories) in a Leucosep[®] filtered tube (227290, Greiner) and centrifuge at $1000 \times g$ for 30 seconds at room temperature.
- Clamp the LRS chamber on a flask support stand and cut the ends of the chamber with sterilized scissors. Perfuse the chamber with HBSS (Hank's BSS, H15-009, PAA Laboratories) into the prepared Leucosep[®] tube up to 50 ml.
- Centrifuge the tube at $450 \times g$ for 30 min (Brake: 0, Acceleration: 1) at room temperature.
- Transfer the ring like section with leucocytes in a new 50 ml Falcon-tube and fill HBSS up to 50 ml.
- Centrifuge the tube at $250 \times g$ for 15 min at room temperature.
- Remove the supernatant and resuspend the pellet in 1-3 ml lysis buffer (155 mM NH_4Cl , 10 mM KHCO_3 , 13 mM EDTA, pH 7.3) to lyse the erythrocytes.
- Keep the cells in the lysis buffer for 1 minute and then immediately fill HBSS up to 50 ml.
- Centrifuge the tube at $130 \times g$ for 10 min at room temperature.
- Remove the supernatant and resuspend the pellet in 20 ml cold 0.5 % BSA/PBS.

3.2.2 CD8⁺ T cell isolation

To get SEA (Staphylococcal Enterotoxin A)-specific CTLs, purified lymphocytes were stimulated with SEA (5 µg/ml, S-9399, Sigma) in AIMV medium (12055, Invitrogen) at a density of 1×10^8 cells/ml, at 37°C for 1 hr. After that, stimulated PBLs were re-suspended at a density of 2×10^6 cells/ml in AIMV medium supplemented with 10% FCS and 100 U/ml of recombinant human IL-2 (PHC0021, Biosource). After 5 days, SEA-specific CTLs were positively isolated using a Dynal[®] CD8 positive isolation kit (113.33D, Invitrogen). Purified SEA-specific CTLs were then maintained in AIMV medium supplemented with 10 % FCS and 100 U/ml of recombinant human IL-2. The CTLs from day 2 to day 3 after positive isolation were used for experiments.

For TIRF microscopy and live cell imaging, naïve CD8⁺ T cells were isolated from PBLs using a CD8 negative isolation kit (Dynabeads[®] Untouched[™] Human CD8 T Cells, 113.48D, Invitrogen) and one day after isolation the CD8⁺ T cells were stimulated with Dynabeads[®] Human T-Activator CD3/CD28 (111.31D, Invitrogen).

3.2.3 Cell culture

Naïve CD8⁺ T cells were maintained in at a density of 3×10^6 cells/ml in AIMV medium supplemented with 10% FCS (10270-106, Invitrogen) and CTLs were maintained at a density of 1×10^6 to 4×10^6 cells/ml in AIMV medium supplemented with 10% FCS and 100 U/ml of recombinant human IL-2.

Raji cells (CCL-86[™], ATCC) were maintained in RPMI 1640 medium (21875, Invitrogen) supplemented with 10% FCS.

3.3 Electroporation of CD8⁺ T cells

For SEA-specific CTLs, 1 day after positive isolation cells (5×10^6 to 6×10^6 cells for one transfection) were collected and washed once with pre-warmed 0.5% BSA/PBS by low speed centrifugation ($100 \times g$, 8 min). AIMV medium was plated in a12-well plate and pre-incubated in the incubator for 30 min before transfection to equilibrate CO₂. The cells were electroporated with siRNA using the Human T cell nucleofactor kit (VPA-1002, Lonza) with the program T-023 in Amaxa Nucleofactor™ II. Afterwards the cells were maintained in CO₂-preequilibrated AIMV medium (containing 10% FCS, 1.5 ml for one transfection). 12 hours after electroporation, the dead cells were removed by low speed centrifugation ($100 \times g$, 8 min) and fresh AIMV medium (containing 10% FCS and 50U/ml IL-2, 3.5 ml for one transfection) was given to the cells. 36 hours after electroporation the cells were used for experiments.

For CD3/CD28 bead-stimulated CD8⁺ T cells, 3 days after stimulation the beads were removed by the magnet. Cells (5×10^6 cells for one transfection) were collected and washed once with pre-warmed 0.5% BSA/PBS by low speed centrifugation ($100 \times g$, 8 min). The cells were then electroporated with 1.5 µg of perforin-mCherry (or siRNA and perforin-mCherry) using the Human T cell nucleofactor kit with the program T-023 in Amaxa Nucleofactor™ II. Afterwards the cells were maintained in CO₂-preequilibrated AIMV medium (containing 10% FCS, 1.5 ml for one transfection). 6 hours after electroporation, the dead cells were removed by low speed centrifugation ($100 \times g$, 8 min) and fresh AIMV medium (containing 10% FCS, 2 ml for one transfection) was given to the cells. 24 to 30 hours after electroporation the cells were used for experiments.

3.4 Construction of cDNA

Perforin was amplified from human cDNA with primers 5' TAT ATA AGA TCT CCA CCA TGG CAG CCC GTG TGC TCC and 5' TAT ATA TAC CGG TGG CCA CAC GGC CCC ACT CCG G to add Bgl2 and Age1 restriction sites at each end. The mCherry construct was obtained as a gift from Roger Tsien. After Age1 and Bgl2 restriction digestion, perforin was ligated to mCherry at its C-terminus and then purified.

3.5 Labeling recycling TCR in live cells

To specifically label endocytosed TCR and plasma membrane TCR, CTLs were first incubated with Alexa⁴⁸⁸-labeled anti-CD3 mAb in AIMV medium at 37 °C for 30 min. The cells were then put on ice and the remaining surface labeling was removed by washing the cells twice for 1 min with ice-cold acid medium (RPMI [Invitrogen], 25 mM sodium acetate [pH 2]), followed by neutralization with RPMI (pH 10). After that the cells were incubated with Alexa⁶⁴⁷-labeled anti-CD3 mAb in AIMV medium on ice for 1.5 hr to label plasma membrane TCR. Same procedure described above was followed to make the conjugation of CTLs to target cells.

3.6 Immunofluorescence

Raji cells were pulsed with 10 µg/ml of SEA in AIMV medium (10% FCS) at 37°C for 30 min. CTLs were incubated with Alexa⁴⁸⁸-labeled anti-CD3 mAb at 37°C for 30 min to label rTCR. After that CTLs and SEA-pulsed Raji cells were harvested and washed once with fresh AIMV medium by centrifugation at 200 × g for 5 min. The supernatant was then

3. Materials and methods

removed and cells were resuspended at a density of 2×10^7 cells/ml in AIMV medium. CTLs and Raji cells were mixed at a ratio of 1:1 and this cell suspension were incubated at 37 °C for 5 min. After that the cell suspension was diluted to a density of 4×10^6 cells/ml and plated onto poly-ornithine pre-coated glass coverslips and incubated at 37 °C for the time specified in the figure legends. Samples were then fixed with ice-cold 4% of paraformaldehyde for 20 min and processed for immunofluorescence as follows:

- Wash the samples once with 0.1M Glycine (in PBS) for 3 min;
- Remove glycine buffer and incubate the samples with 0.1% Triton/PBS buffer for 15 min to permeabilize the cells;
- The samples were then incubated with blocking buffer (2% BSA, 0.1% Triton/PBS) for 15 min to block the unspecific binding sites in the samples;
- Afterwards the primary antibody (1:50 to 1:500 in blocking buffer, depending on the antibody) was given to the samples for 1.5 hours at room temperature or overnight at 4 °C; then the primary antibody was removed and the samples were washed with 0.1% Triton/PBS for 3 times;
- Afterwards the secondary antibody (1:2000 in blocking buffer) was given to the samples for 45 min at room temperature; then the antibody was removed and the samples were washed with 0.1% Triton/PBS twice and with PBS once;
- The samples were carefully mounted in the mounting medium.

3.7 Confocal microscopy

Confocal microscopy was carried out on a Nikon E600 using a 100× objective in the Department of Cell Biology (Prof. Peter Lipp). Serial confocal z-sections were taken at 0.2 μm intervals for whole cell analysis. Normally 30 to 40 slices were taken for each cell which contained all the three-dimensional fluorescence information. Detectors were set to detect an optimal signal below the saturation limits. Image sets to be compared were acquired during the same session and using the same acquisition settings. Interaction between lytic granules and recycling TCR compartments was quantified through the z-sections, meaning that both lateral and longitudinal interaction were taken into account. ImageJ 1.37v software was used to generate merged images and projections of confocal sections.

3.8 Epifluorescence deconvolution microscopy and time-lapse imaging

Human CTLs overexpressing perforin-mCherry were incubated with Alexa⁴⁸⁸-labeled anti-CD3 mAb at 37 °C for 30 min. 4D fluorescence microscopy was performed with a Zeiss Cell Observer HS system with a 100× alpha Plan-Fluar Objective (N.A. 1.45) and an AxioCam MRm Rev. 3. The filter set was a Zeiss 62 HE tripleband with single excitation filters inside the fast-wavelength switching xenon burner DG-4 (Sutter Instruments). For fixed cells, images were acquired with binning 1 × 1 and a z-stepsize of 0.2 μm. For time-lapse imaging, to acquire the images as fast as possible, the cells were scanned with binning 3 × 3 and a z-stepsize of 1 μm. Iterative deconvolution was performed using a point spread function (PSF) calculated with the z-stack acquisition from a 170 nm fluorescent bead (Tetraspeck, Invitrogen).

3.9 Evanescent-wave imaging

A TIRF setup as described¹⁶⁹ was used with the following additions: a solid-state laser 85 YCA emitting at 561nm (Melles Griot), a dual-view camera splitter (Visitron) to separate the red and green channels, a Visichrome Monochromator (Visitron) to acquire images in epifluorescence. Human CTLs overexpressing perforin-mCherry were washed and allowed to settle for 2 min on anti-CD3/anti-CD28 antibody-coated coverslips. Cells were imaged for 30 min by TIRFM at 561 nm. To distinguish between secretion of LG and movement of granules from the plasma membrane inside the cell, we also recorded the cell in epifluorescence at 561 nm. Following each TIRF image, three images were acquired as epifluorescence stacks with a z-stepsize of 0.5 μ m, the first epifluorescence plane being at the same plane as that of TIRFM. For experiments with paired vesicles, cells were pre-incubated with Alexa⁴⁸⁸-conjugated anti-CD3 mAb at 37 °C for 30 min and then were settled on anti-CD3/anti-CD28 antibody-coated coverslips as described above. Cells were imaged for 20 min by TIRFM at 488 and 561 nm. Since the granules never moved 1.0 μ m above the TIRF plane and for faster imaging with two lasers, following each TIRF image, only two images were acquired in epifluorescence at 561 nm, one at the same plane as that of TIRFM and the second image at 0.75 μ m above the TIRF plane. The acquisition speed was 1 Hz and the exposure time was 100 ms.

3.10 Lytic granule accumulation analysis

The analysis of lytic granule accumulation was performed with Metamorph version 6.3. The raw data stacks were first corrected for background and then a threshold value was set for every cell such that only the pixels above a given fluorescence intensity that mark the

lytic granules were selected. The value of the pixels defined as the threshold area was obtained for every frame of the time lapse movie for each individual cell. Due to difficulties in tracking every single vesicle for all the cells, a ratio was made between the threshold area and number of vesicles for a minimum of three frames for every cell. The area threshold was then divided by this ratio for all the time frames to get the number of vesicles for each frame. The average of the number of vesicles was then plotted against the time in seconds.

3.11 Small interfering RNA (siRNA)

All siRNA used in this study were modified by Qiagen as described by Mantei *et al.*¹⁷⁰. SEA-specific CTLs were transfected with modified siRNA designed to silence human *vti1b* (VTi1B_8_4479, Qiagen) using nucleofector kit (Lonza) according to the manufacturer's instructions. A modified non-silencing siRNA (A3617/18S, Qiagen) was used as control. Fresh AIMV medium containing 50 U/ml recombinant human IL-2 was given to the cells 12 hours after transfection. The cells were then kept in culture for additional 24 hours before use.

3.12 RealTime-PCR

For Quantitative RealTime-PCR (qRT-PCR), total RNA was isolated using TRIzol® Reagent (15596018, Invitrogen) including 1 µl Glycogen (5 µg/µl, 10814-010, Invitrogen) according to the manufacturer's protocol as follows:

3. Materials and methods

- Harvest cells ($1-1.5 \times 10^6$ cells for each sample) by centrifugation at $200 \times g$ for 5 minute and then add 800 μ l TRIzol to the pellet;
- Centrifuge at $12,000 \times g$, 10 min at room temperature;
- Transfer the supernatant to a fresh eppendorf tube and incubate for 5 min at room temperature;
- Add 0.2 ml of Chloroform and shake vigorously for about 15 seconds;
- Leave the samples at room temperature for 2-3 min;
- Centrifuge at $12,000 \times g$, 15 min at 4 °C;
- Transfer the aqueous phase to a fresh tube and add 1 μ l Glycogen (5 μ g/ μ l);
- Add 0.5 ml of Isopropanol and incubate for 10 min at room temperature;
- Centrifuge at $12,000 \times g$, 10 min at 4 °C;
- Remove the supernatant and add 1 ml of 75% Ethanol (in DEPC-treated H₂O);
- Centrifuge at $7,500 \times g$, 5 min at 4 °C;
- Leave the RNA pellet dry at room temperature and then dissolve RNA in 10 μ l of DEPC-treated H₂O;
- Determine the concentration of RNA using 2% Agarose gel.

0.8 μ g total RNA was then reverse transcribed into cDNA by SuperScript™ II reverse transcriptase (18064-014, Invitrogen) including 1 μ l RNaseOut, (10777-019, Invitrogen) and 1 μ l oligo dT Primer (0.5 μ g/ μ l, 18418-012, Invitrogen) following the manufacturer's instruction. RealTime PCR was carried out in a MX3000 instrument from Stratagene. 1.0 μ l cDNA and 300 nM of each primer were set into PCR reactions (25 μ l) using Quanti Tect SYBR green kit (204145, Qiagen). PCR conditions were: initial denaturation, 15 min, 94 °C; 45 cycles: denaturation, 30 s, 94 °C; annealing, 45 s, 58 °C; elongation, 30 s, 72 °C

and finally a dissociation curve cycle (60 s, 95 °C; 30 s 55 °C; 30 s 95 °C). Primers were designed using Primer3 program ¹⁷¹ available at <http://frodo.wi.mit.edu/>. PCR fragments were confirmed by sequencing (MWG).

3.13 Western blotting

CTLs were collected 36 hours after siRNA transfection. The cells (1.5×10^7 cells for each sample) were collected and washed once with PBS before putting in SDS loading buffer containing 1% β -mercaptoethanol (50 μ l for each sample). Afterwards the cells were disrupted and homogenized by sonication. The samples were then incubated at 95°C for 5 min. Equivalent amounts of proteins were separated by 12% Tris-Glycine SDS-PAGE gels and transferred to nitrocellulose membrane using X-Cell II (Invitrogen). ECL reagent (34076, Pierce) was used for immunoblot detection.

3.14 Cytotoxicity assay

The CytoTox 96[®] Non-Radioactive Cytotoxicity Assay (G1780, Promega) was used to detect target lysis. SEA-specific CTLs were plated in 96-well plates in AIMV medium (5% FCS) with 1×10^4 SEA-pulsed Raji target cells in each well at various effector/target ratios (the experimental reactions). CTLs and SEA-pulsed Raji target cells were then incubated at 37 °C for 4 hours and the Lactate dehydrogenase activity in the supernatant was measured. The cells were spun down at 200 g for 4 min. 50 μ l of supernatant from each well was transferred into a new black 96-well plate with clear flat-bottom (353948, BD Biosciences). The supernatant was incubated with the reaction substrate (50 μ l for each well) for 30 min at room temperature. The reaction was ceased by adding the stop solution (50 μ l for each

3. Materials and methods

well). The absorbance was measured at 490 nm with the GENios-Pro plate reader (TECAN). Control reactions were set as follows:

- Effector Cell Spontaneous LDH Release: Add effector cells at each concentration used in the experimental setup to wells containing AIMV medium (5% FCS). The final volume was adjusted to the same as in the experimental wells.
- Target Cell Spontaneous LDH Release: Add target cells (1×10^4 in each well) to wells containing AIMV medium (5% FCS). The final volume was adjusted to the same as in the experimental wells.
- Target Cell Maximum LDH Release: Add target cells (1×10^4 in each well) to wells containing AIMV medium (5% FCS). The final volume was adjusted to the same as in the experimental wells. 45 min prior to harvesting the supernatants from experimental reactions, 10 μ l of the Lysis Solution (10 \times) was added to each well.
- Volume Correction Control: Add 10 μ l of Lysis Solution (10 \times) to a triplicate set of wells containing 100 μ l of AIMV medium (5% FCS). This control is used to correct for the volume increase caused by the addition of Lysis Solution (10 \times).
- Culture Medium Background: Add 100 μ l of AIMV medium (5% FCS) to a triplicate set of wells.

Each experimental and control reaction was performed in triplicate. To calculate the results, we first subtracted the average of absorbance values of the Culture Medium Background from all absorbance values of experimental and control reactions. The volume change of the Target Cell Maximum LDH Release was then corrected by subtracting the average of the Volume Correction Control. Use these corrected values in the following formula to compute percent cytotoxicity for each effector : target cell ratio.

% Cytotoxicity = (Experimental – Effector Spontaneous – Target Spontaneous) / (Target Maximum – Target Spontaneous) × 100.

3.15 Data analysis

Data were analyzed using ImageJ 1.37v, Metamorph (Visitron), AxioVision (Zeiss), Igor Pro (Wavemetrics), Microsoft Excel (Microsoft) and SigmaPlot 8.0. All values are given as mean ± S.E.M if not mentioned otherwise. In case, data points were normally distributed, an unpaired two-sided student t-test was used. If normal distribution could not be confirmed, a non-parametric test (Mann-Whitney) was performed. P-values are stated in the figure legends. * P<0.05, ** P<0.01, *** P<0.005.

4. Results

4.1 LG were tethered with rTCR

4.1.1 Recycling TCR was not in the position to trigger downstream signaling

Previous reports have shown that TCR recycling is essential for TCR enrichment at the IS after target cell recognition¹⁰⁴⁻¹⁰⁶. It's reasonable to assume that recycling TCR are involved in recruiting effector molecules and triggering downstream signaling pathways. We first characterized the kinetics of the recycling TCR translocation to the the IS. We labelled recycling TCR by pre-incubation of Alexa⁴⁸⁸-conjugated anti-CD3 antibody with CTLs at 37°C for 30 minutes. Afterwards the antibody remaining on the cell surface was washed away, followed by labelling cell surface TCR with Alexa⁶⁴⁷-conjugated anti-CD3 antibody. Then the CTLs were incubated with target cells — SEA-pulsed Raji cells — to form the CTL-target cell conjugates. Afterwards the CTL-target cell conjugates were fixed with ice-cold 4% of paraformaldehyde (PFA). We found that the TCR initially enriched at the IS were the plasma membrane TCR. Whereas, most of the recycling TCR unexpectedly approached the IS only at later time points, between 15 min and 30 min after target cell recognition (Fig. 1A). This result suggests that recycling TCR enrichment at the IS is not necessary to recruit effector molecules to the IS and initiate downstream signalling pathways immediately after target cell recognition.

4. Results

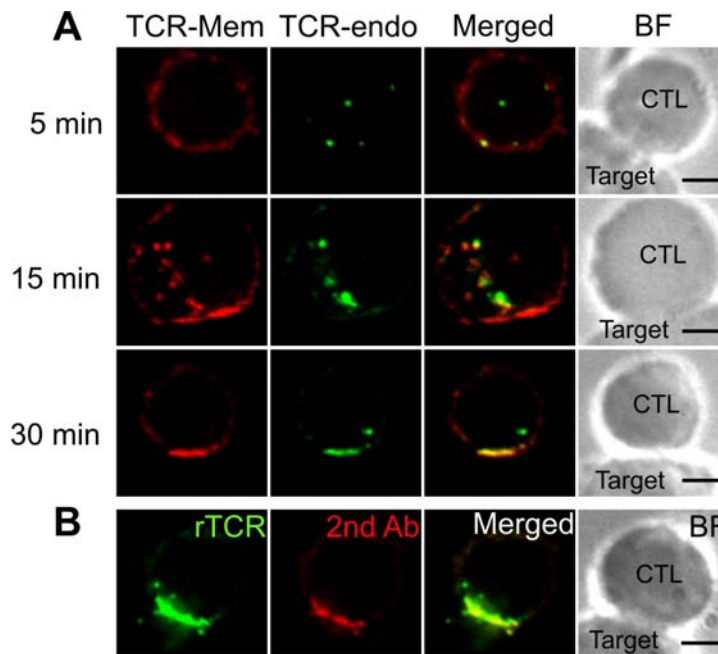


Figure 1. The initial TCR enrichment at the IS was not initiated by rTCR. (A) TCR on the surface initiates IS formation. Endocytosed TCR (TCR-endo, green) was labeled with Alexa⁴⁸⁸-labeled anti-CD3 mAb. TCR remaining on the cell surface (TCR-Mem, red) was labeled by Alexa⁶⁴⁷-labeled anti-CD3 mAb. BF, bright field. (B) The recycling TCR (green) was labeled with Alexa⁴⁸⁸-labeled anti-CD3 mAb. Among the TCR accumulated at the IS, only some were incorporated into plasma membrane, which were labeled by Alexa⁵⁶⁸ secondary Ab under nonpermeabilizing conditions (red). Scale bars are 3 μ m.

To analyze whether recycling TCR were incorporated into the plasma membrane and could thus be involved in maintaining signaling, we examined the localization of recycling TCR at the IS with the following staining protocol using confocal microscopy. The recycling TCR were pre-labelled by of Alexa⁴⁸⁸-conjugated anti-CD3 antibody in live CTLs. To determine the recycling TCR incorporated into the plasma membrane, we stained the samples (30 minutes after contact) with Alexa⁵⁶⁸-conjugated secondary antibody without permeablizing the cells. We found that only a small fraction of the TCR, which were recycled to the IS, were incorporated into the plasma membrane (Fig. 1B), indicating that

recycling TCR may have other functions apart from triggering or maintaining downstream. This raises the question why there is a robust TCR enrichment at the IS, if most of receptors are not incorporated into the plasma membrane to trigger downstream signalling. To address this question we examined alternative functions of recycling TCR.

4.1.2 Lytic granules were localized next to recycling TCR

After CTLs recognize target cells, lytic granules are reorientated and accumulated at the IS. The transport, docking and release of lytic granule at the IS are required for effective target cell killing⁹, while dysfunction of lytic granule release is associated with life-threatening familial or acquired hemophagocytic lymphohistiocytosis¹⁷². Lytic granules and recycling TCR are located in distinct compartments and no evidence has been shown that there is a common mechanism to transport them to the IS. To explore whether the transport and/or accumulation of recycling TCR and lytic granules was linked in any way, we examined the localization of lytic granules and recycling TCR. We pre-incubated Alexa⁴⁸⁸-conjugated anti-CD3 antibodies with CTLs to label the recycling TCR. Then the CTLs were incubated with target cells to form the conjugates. Afterwards the CTL-target cell conjugates were fixed at various time points. Unexpectedly, we found that many lytic granules were paired/tethered with recycling TCR in both resting and activated CTLs (Fig. 2A).

We subsequently examined the lytic granule/recycling TCR (LG/rTCR) pairing rate at different CTL states after target cell recognition. The analysis showed that in the resting state, the LG/rTCR pairing rate was already considerably high; during IS maturation, the LG/rTCR pairing rate was higher than 80% (Fig. 2B). This high level of compartment pairing suggests that recycling TCR play an important role in the function of lytic granules at the IS.

4. Results

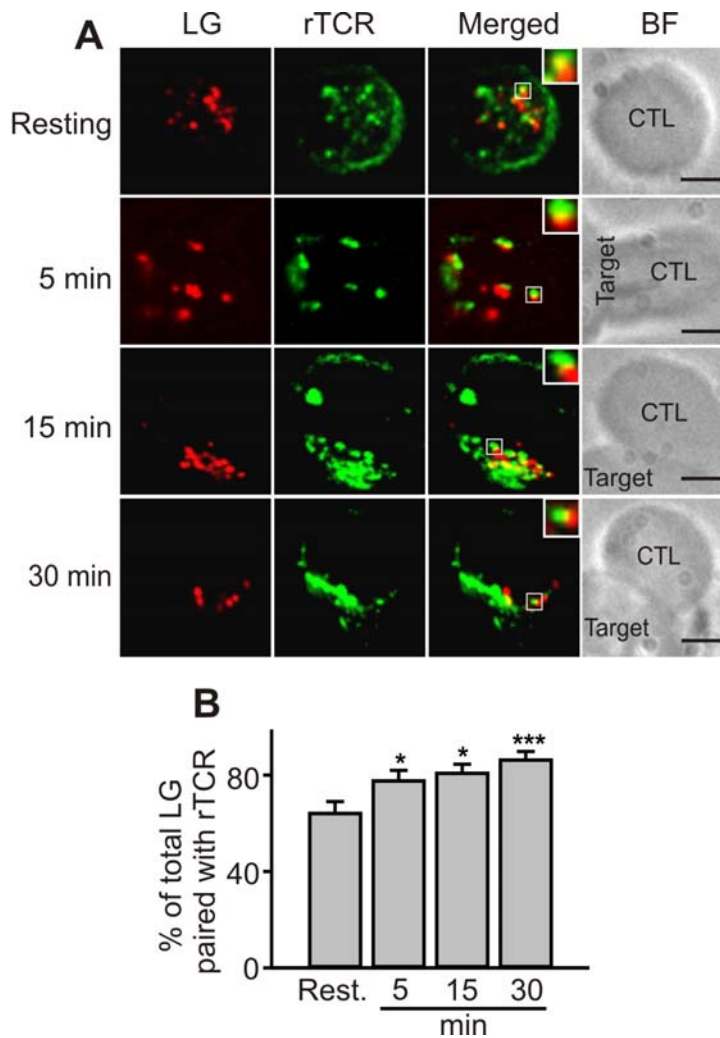


Figure 2. LG are localized next to rTCR. (A) CTLs were pre-incubated with Alexa⁴⁸⁸-labeled anti-CD3 mAb to label rTCR. Perforin was used as the LG marker. In both resting CTLs and CTLs in contact with target cells, LG (red) were next to rTCR (green). (B) The possibility of tethering LG with rTCR is high before and after IS formation. For resting, 5 min, 15 min and 30 min, 215, 170, 221 and 145 LG were analyzed.

To exclude that lytic granules and recycling TCR were in fact colocalized but not paired/tethered, we performed two types of control experiments. Fig. 3A shows the staining of recycling TCR with Alexa⁶⁴⁷- and Alexa⁴⁸⁸-conjugated anti-CD3 antibodies.

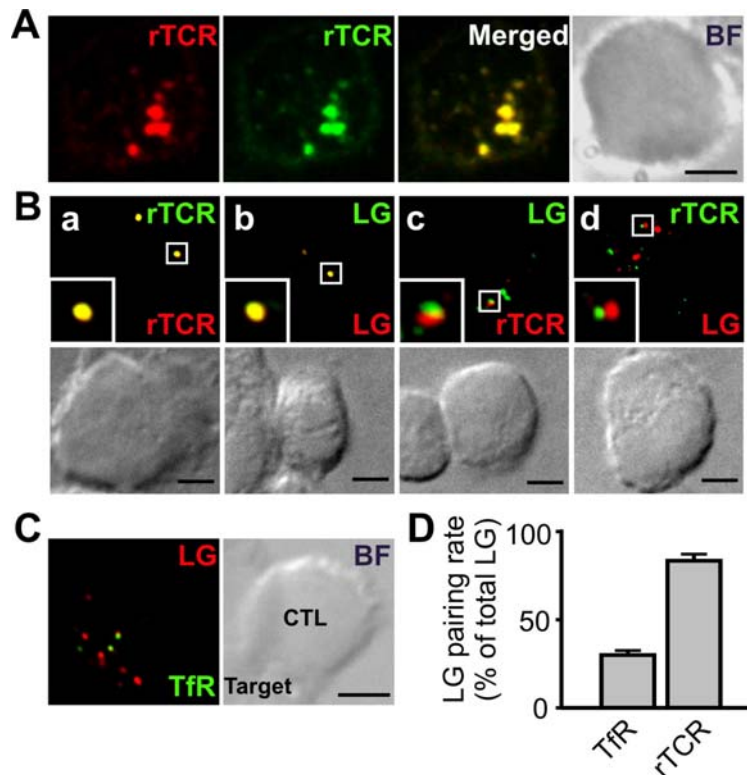


Figure 3. Tethering of LG and rTCR is specific. (A) Confocal analysis of TCR labeled with Alexa⁴⁸⁸- and Alexa⁶⁴⁷-labeled anti-CD3 mAb. (B) Pairing is distinct from co-localization. rTCR were labeled with Alexa⁴⁸⁸-labeled anti-CD3 mAb in **a** and **d**, as well as Alexa⁶⁴⁷-labeled anti-CD3 mAb in **a** and **c**. LG were labeled with Alexa⁶⁴⁷-labeled anti-perforin mAb in **b** and **d**, as well as FITC-labeled anti-perforin mAb in **b** and **c**. Images were taken with the Zeiss Cell Observer and deconvoluted with the corresponding PSF. (C) Localization of lytic granules relative to endocytosed Tfr compartments. Prior to conjugation with SEA-pulsed Raji cells, CTLs were incubated with Alexa⁴⁸⁸-Tfr at 37 °C for 30 min to label the endocytosed Tfr. LG were labeled with Alexa⁶⁴⁷-labeled anti-perforin mAb. Scale bars are 3 μm. (D) The rate of lytic granule pairing with endocytosed Tfr and rTCR.

In contrast to the juxtaposition of lytic granules and rTCR shown in Figure 1B, a perfect co-localization of both anti-CD3 antibodies was observed by confocal microscopy as expected (Fig. 3A) because both antibodies stain the same protein and are thus localized in

4. Results

the same compartments. Co-localization of proteins can therefore be clearly distinguished from proteins that are juxtapositioned.

Moreover, we verified colocalization versus pairing using epifluorescence deconvolution microscopy. Four combinations of staining of lytic granules and recycling TCR were examined: (a) Alexa⁶⁴⁷- and Alexa⁴⁸⁸-conjugated anti-CD3 antibodies, (b) Alexa⁶⁴⁷- and FITC-conjugated anti-perforin antibodies, (c) Alexa⁶⁴⁷-conjugated anti-CD3 and FITC-conjugated anti-perforin antibodies, (d) Alexa⁴⁸⁸-conjugated anti-CD3 and Alexa⁶⁴⁷-conjugated anti-perforin antibodies (Fig. 3B). As expected, the control double staining of recycling TCR or lytic granules showed a clear colocalization (Fig. 3B a, b). However, the two separate staining conditions of lytic granules and recycling TCR (Fig. 3B c, d) showed no colocalization but some LG/rTCR pairs. This demonstrates that lytic granules and recycling TCR can form pairs in CTLs. Given the fact that more than 60% lytic granules are paired with recycling TCR in resting CTLs and that this number increases during IS maturation, we propose that the pairing of lytic granules and recycling TCR is important for the function of lytic granules.

To prove the specificity of pairing between eTCR and LG, we compared the localization of LG and the endocytosed transferrin receptor as a control. Transferrin is recycled through the constitutive recycling pathway¹⁷³⁻¹⁷⁴. Using Alexa⁴⁸⁸-conjugated transferrin to label recycling transferrin receptors (TfR), we observed only infrequent pairing between lytic granules and the endocytosed TfR (Fig. 3C). This pairing was on average less than 30% in contrast to the 80% pairing between lytic granules and rTCR (Fig. 3D). We conclude that lytic granules pair with recycling TCR compartments and not with constitutively recycling endosomes.

4.1.3 Paired lytic granules are preferentially accumulated at the IS

Since the accumulation and release of lytic granules at the IS are the two critical steps for executing lytic granule function in CTLs, we first examined whether lytic granule accumulation at the IS is affected by LG/rTCR pairing. We quantified the localization of single and paired lytic granules in CTLs at various time points. As shown in Fig. 4 left image, we divided the CTL evenly in diameter into three parts and defined the part closest to the IS as *in proximity to the IS* (P). If we assume CTLs are sphere-shaped, the volume of P part should be 25.9 % of the total volume of the cell according to the sphere-volume formula. In other words, if granules are randomly distributed in cells, there should be about 25.9 % of the granules in the P part. In resting CTLs the distribution of single and paired lytic granules was very close to this number, suggesting that there was no preferential accumulation of single or paired lytic granules in the resting CTLs (Fig. 4). However, upon time after CTLs contacted with target cells, the percentage of paired lytic granules in proximity to the IS was significantly enhanced, whereas not much change occurred regarding the localization of single lytic granules (Fig. 4). This data indicates that the probability of lytic granule accumulation at the IS is increased by pairing lytic granules with recycling TCR.

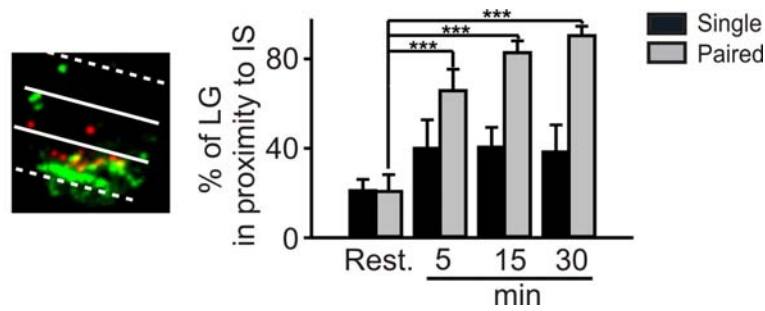


Figure 4. Paired LG were preferentially accumulated at the IS. LG in proximity to the IS were analyzed at various time points. Recycling TCR was labeled with Alexa⁴⁸⁸-conjugated anti-CD3 mAb (green). LG was labeled with Alexa⁶⁴⁷-conjugated anti-perforin mAb (red). The CTL was divided evenly in diameter into three parts as shown above. The part closest to the IS was defined as *in proximity to the IS*. (from lower dashed line to the lower solid line). Rest., resting CTLs. We analyzed 76, 37, 47 and 33 single LG and 159, 115, 134 and 157 paired LG for resting, 5 min, 15 min and 30 min, respectively.

4.2 Lytic granules are accumulated at the IS by tethering with rTCR

4.2.1 Paired lytic granules have longer dwell time at the IS

The data described above were obtained from the fixed cells, which provided important information about granule movement, but it lacked the information about granule movement in real-time. To visualize the kinetics of vesicle movement, we designed experiments in living CTLs. We used fast 4D fluorescence microscopy to visualize movements of lytic granules and recycling TCR in live cells. To label lytic granules in living cells, CTLs were transfected with mCherry-tagged perforin. The next day after the electroporation, CTLs were pre-incubated with Alexa⁴⁸⁸-conjugated anti-CD3 antibody at 37°C for 30 minutes to label recycling TCR. Subsequently the CTLs were incubated with SEA-pulsed Raji cells. The time-lapse recordings were started right after Raji cells were added.

4. Results

In all CTLs we observed LG/rTCR pairs that were transported to the IS (Fig. 5A). After LG/rTCR pairs reached the IS, more than 80% of these LG/rTCR pairs remained at the IS for longer than 30 seconds. In some CTLs single lytic granules were also transported to the IS. However, 30 seconds after approaching the IS only 20% of these single lytic granules still remained at the IS (Fig. 5B). These data show that lytic granules and recycling TCR can be transported together to the IS as LG/rTCR pairs and that tethering with recycling TCR increases the dwell time of lytic granules at the IS.

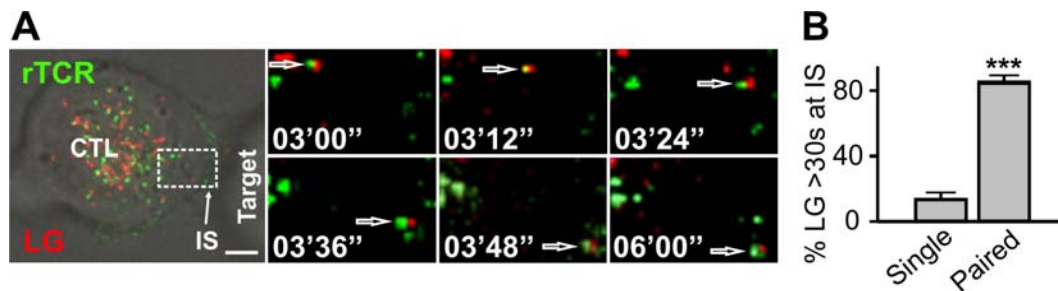


Figure 5. Tethered LG and rTCR were transported to the IS. CTLs overexpressing perforin-mCherry were incubated with Alexa⁴⁸⁸-labeled anti-CD3 mAb to label rTCR. A time-lapse recording was made every 5 seconds with a Zeiss Cell Observer HS system. One exemplary trace of tethered LG and rTCR moving to the IS is shown in (A). After approaching the IS, the percentage of single and paired LG which stayed at the IS longer than 30 s is shown in (B), 26 cells were analyzed.

To analyze the dwell times of lytic granules at the IS in more detail, we used the total internal reflection fluorescence (TIRF) microscopy technique, which allows exclusive visualization of granules within about 200 nm of the IS. To apply TIRF microscopy, a functional IS was formed between CTLs and anti-CD3/anti-CD28 antibody-coated glass coverslips¹⁶⁹.

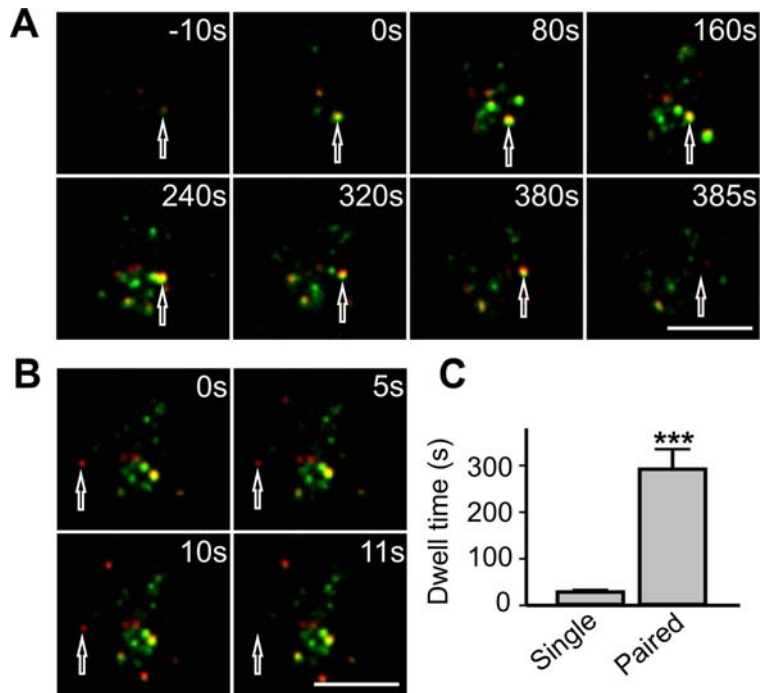


Figure 6. Paired LG have longer dwell times at the IS. LG (red) were marked with perforin-mCherry and rTCR (green) were labeled by pre-incubation the CTLs with Alexa⁴⁸⁸-labeled anti-CD3 mAb. Then LG and rTCR were visualized by TIRF microscopy. Exemplary traces of LG paired with rTCR (**A**) or without rTCR (**B**) are shown. Note the different time scale reflecting the dwell time of the LG at the IS. (**C**) Quantification of the dwell time of individual LG at the IS. Single LG, n = 12; Paired LG, n = 19. Scale bars are 3 μ m.

As described for the 4D-time-lapse imaging, we labeled the lytic granules and recycling TCR with overexpressing mCherry-Perforin and Alexa⁴⁸⁸-conjugated anti-CD3 antibody, respectively. We found that most lytic granules reached the IS being paired with recycling TCR, and paired lytic granules resided at the IS much longer than single lytic granules (Fig. 6A, B). On average, the dwell times of paired lytic granules were ten times longer than dwell times of single lytic granules (Fig. 6C). This finding further supports the hypothesis that tethering with recycling TCR is required for stabilizing/docking lytic granules at the IS. As a consequence, we predict that lytic granule release should be increased accordingly.

4.2.2 Paired lytic granules were secreted preferentially over single lytic granules

In order to determine the influence of LG/rTCR pairing on vesicle release, we established an assay to analyze exocytosis of lytic granules in CTLs. Fig. 7A shows an example of secreted lytic granules. To confirm that a lytic granule was indeed secreted rather than simply having moved away from the TIRF plane, three consecutive epi-fluorescence images were acquired after every TIRF image, in order to determine vesicle movement away from the membrane back into the cytosol. The image series were taken every 1 second for 20 minutes. If a granule disappeared from the TIRF plane and was also not found in the epi-fluorescence images, it had to be secreted (Fig. 7A). In contrast, if a granule disappeared in the TIRF plane, but was still seen in the epi-fluorescence images, it indicates that this granule has just moved away from the interface and back into the cytosol (Fig. 7B).

Using this assay, we found that the average dwell times of the secreted lytic granules were drastically increased compared with the dwell times of non-secreted lytic granules (Fig. 7C). This also implies that it is necessary for lytic granules to reside at the IS for a notably long time in order to prime and/or dock at the plasma membrane before undergoing the fusion process.

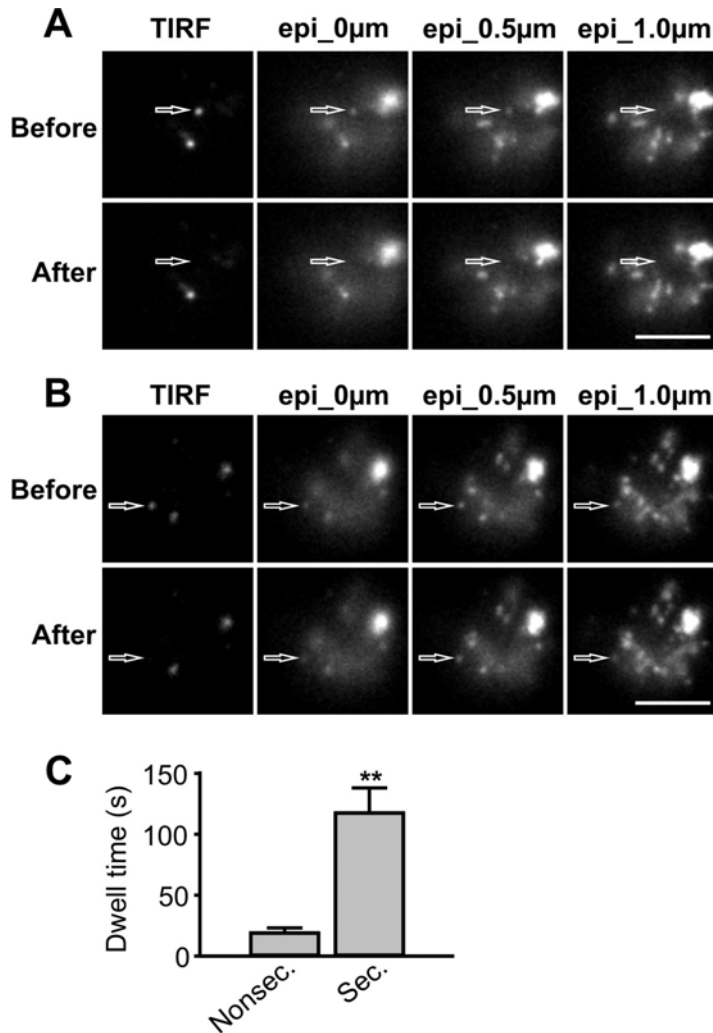


Figure 7. Distinguishing secretion from movement back into the cytosol. (A) TIRF and epifluorescence images taken at planes 0, 0.5 and 1.0 μm above the TIRF plane, before and after secretion. The LG (marked by an arrow), which was secreted, was neither present in the TIRF image nor in the epifluorescence stack images in the *After* panel. (B) A LG moved away from the TIRF plane. In the *After* panel the LG was not seen in the TIRF image, but was still visible in the epifluorescence images. Scale bars are 3 μm . (C) Dwell times of nonsecreted (Nonsec. $n = 20$) and secreted LG (Sec. $n = 14$).

Next, we used this assay to examine the release of paired and single lytic granules. Fig. 8A shows the release of a paired lytic granule. On average, 88% of the released lytic granules

were paired (Fig. 8B). Furthermore, within the first 7 minutes after IS formation, all secreted lytic granules were paired with recycling TCR compartments. Given the results presented in Figs. 6-8 (that both secreted lytic granules and paired lytic granules have long dwell times and additionally paired lytic granules were secreted preferentially over single lytic granules), we conclude that pairing with recycling TCR stabilizes lytic granules at the IS and thus increases the probability of lytic granule release.

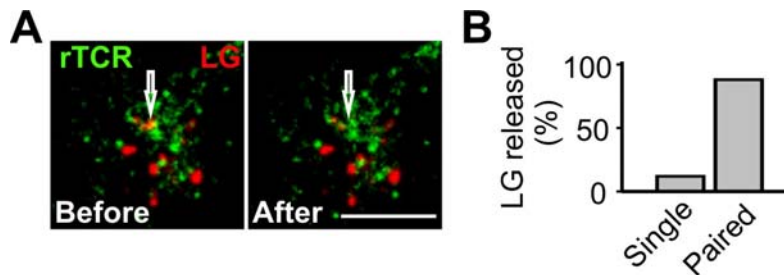


Figure 8. Secretion of the LG paired with rTCR. (A) LG (red) were marked with perforin-mCherry and rTCR (green) were labeled by pre-incubation the CTLs with Alexa⁴⁸⁸-labeled anti-CD3 mAb. Then LG and rTCR were visualized by TIRF microscopy. Three consecutive epi-fluorescence images above TIRF plane were taken to make sure that the granule was secreted other than moving away from TIRF plane. The secreted paired LG is pointed with an open arrowhead. Scale bar is 3 μ m. (B) Analysis of the relative proportion of single and paired LG release at the IS. 20 released vesicles were analyzed.

4.2.3 The Golgi apparatus is involved in LG/rTCR pairing and plays a key role in LG/rTCR transport to the IS

The question we ask next is where the pairing of lytic granules and rTCR takes place. It has been reported that the Golgi apparatus plays a pivotal role in TCR recycling¹⁰⁵ as well as in lysosomal protein processing and sorting¹⁷⁵. In the Golgi apparatus — the harbor for protein sorting and transportation — there are good chances for the lytic granules to meet

4. Results

the recycling TCR. Therefore we examined the location of LG/rTCR pairs and the Golgi apparatus. We found that some LG/rTCR pairs did co-localize with the Golgi apparatus, but many of LG/rTCR pairs did not (Fig. 9). There are two explanations for this observation: either lytic granules pair with recycling TCR in the Golgi apparatus which are then rapidly transported elsewhere, or this pairing may take place not only in the Golgi apparatus but also elsewhere in CTLs.

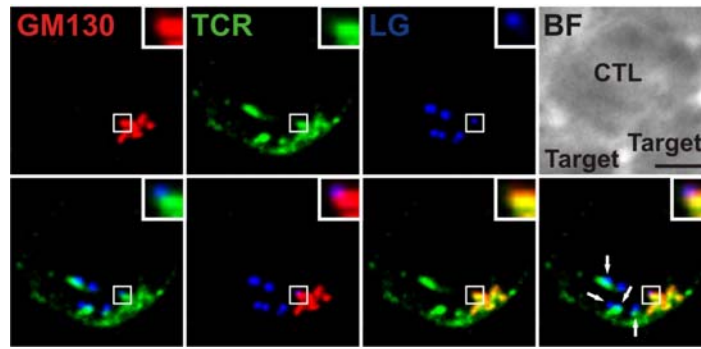


Figure 9. Paired LG are not colocalized with the Golgi marker. LG was labeled with Alexa⁶⁴⁷-conjugated perforin mAb. TCR was stained with Alexa⁴⁸⁸-conjugated CD3 mAb. GM130 was used as the marker for the Golgi apparatus. The merged images are shown in the lower panel. The LG/rTCR pair colocalized with GM130 is enlarged in the insertion. The other LG/rTCR pairs are highlighted by the arrowheads. The scale bar is 3 μ m.

To further analyze the function of the Golgi apparatus for LG/rTCR pairing, we used brefeldin A (BFA) to block functions of Golgi apparatus, by inhibiting the activation of Arf1 by its GEFs in vivo¹⁷⁶. CTLs were pre-treated with BFA for 30 minutes before forming the conjugates with target cells. We found that the pairing rate of lytic granules was reduced when the Golgi apparatus was disassembled by BFA (Fig. 10A and B).

4. Results

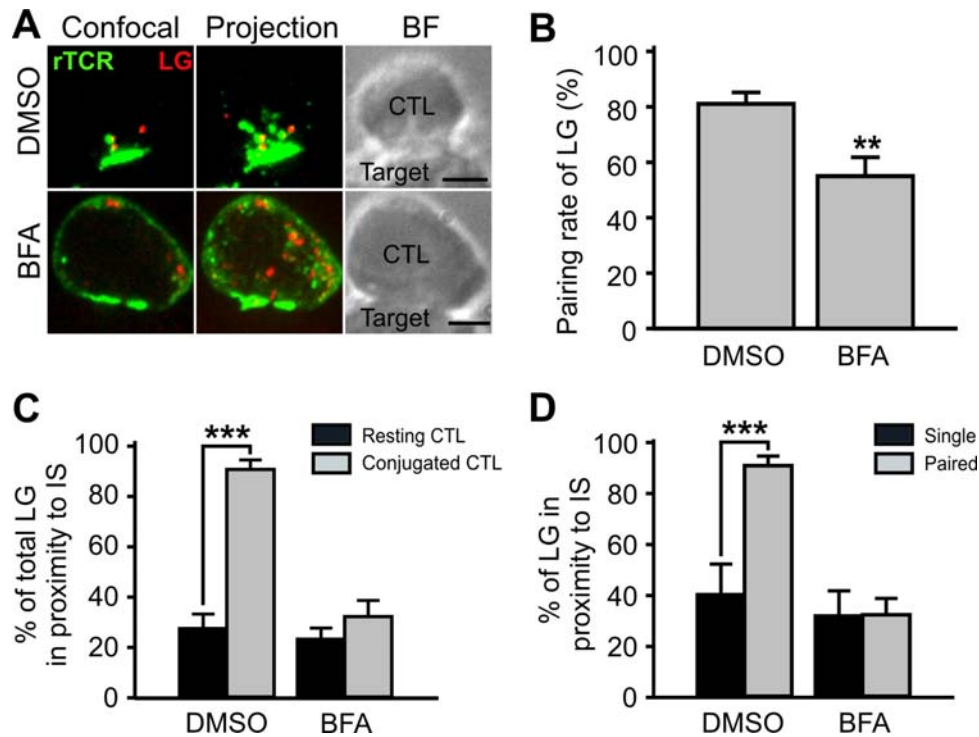


Figure 10. Inhibition of TCR recycling by BFA abolished accumulation of paired LG. (A) CTLs were treated with DMSO or BFA for 30 min at 37°C. LG (red) were marked with Alexa⁶⁴⁷-conjugated perforin mAb and rTCR (green) were labeled by pre-incubation CTLs with Alexa⁴⁸⁸-conjugated anti-CD3 mAb. After 30 min incubation at 37 °C the CTL-target conjugates were fixed with ice-cold 4% PFA. A single plane from the stack is shown in the left panel (Confocal). The projection of the whole stack is shown in the middle panel (Projection). Scale bars are 3 μm. (B) The pairing rate of LG was reduced in BFA-treated CTLs. (C) The accumulation of LG at the IS was abolished by BFA treatment. Resting CTLs were taken as the control for the CTLs conjugated with SEA-pulsed Raji cells for 30 min. (D) The accumulation of paired LG at the IS was abolished by BFA treatment. *In proximity to the IS* was defined as in Fig. 4.

Moreover, lytic granules accumulation at the IS was substantially inhibited in the presence of BFA (Fig. 10C). In particular, the accumulation of paired lytic granules at the IS was completely abolished by BFA treatment, whereas there was no change in single lytic granule distribution (Fig. 10D). These results suggest that the Golgi apparatus is involved

in LG/rTCR pairing; more importantly, the Golgi apparatus plays a key role in the transport of paired lytic granules to the IS and consequently regulates lytic granule accumulation at the IS.

4.3 Vti1b co-localized with paired LG and enhances the possibility for vesicle pairing

4.3.1 Analyzing the co-localization of SNARE proteins with lytic granules and recycling TCR

The next question to be addressed is which protein(s) is (are) responsible for LG/rTCR pairing. SNARE proteins are known to be the key players in intracellular vesicle budding, vesicular transport and vesicle fusion¹³⁷⁻¹³⁹. We therefore examined the localization of SNARE proteins and lytic granules in parallel with TCR. We screened all SNARE proteins against commercially available antibodies at the time. Some examples are shown in Fig. 10. From all the SNARE proteins examined, we found that the Qb-SNARE protein Vti1b co-localized very well with lytic granules and with recycling TCR. In addition, Vti1b also accumulated at the IS after target cell recognition (Fig. 11). Some SNARE proteins examined were also enriched at the IS, such as Qa-SNAREs syntaxin 4 and syntaxin 16, Qb-SNARE Vti1a and Qc-SNARE syntaxin 6. However they didn't show good co-localization either with lytic granules or recycling TCR (Fig. 11).

To further verify the colocalization of Vti1b with both lytic granules and recycling TCR, we investigated various time points after CTLs contact with target cells. We again found that at all the time points Vti1b co-localized very well with lytic granules as well as recycling TCR. Furthermore, Vti1b reorientation to the IS along with lytic granules and

4. Results

recycling TCR during IS maturation was again confirmed (Fig. 12 A and B). Given these results, we formulated the following hypothesis:

1. Vti1b may be involved in accumulation of lytic granules and recycling TCR at the IS
2. Vti1b may play a role in LG/rTCR pairing

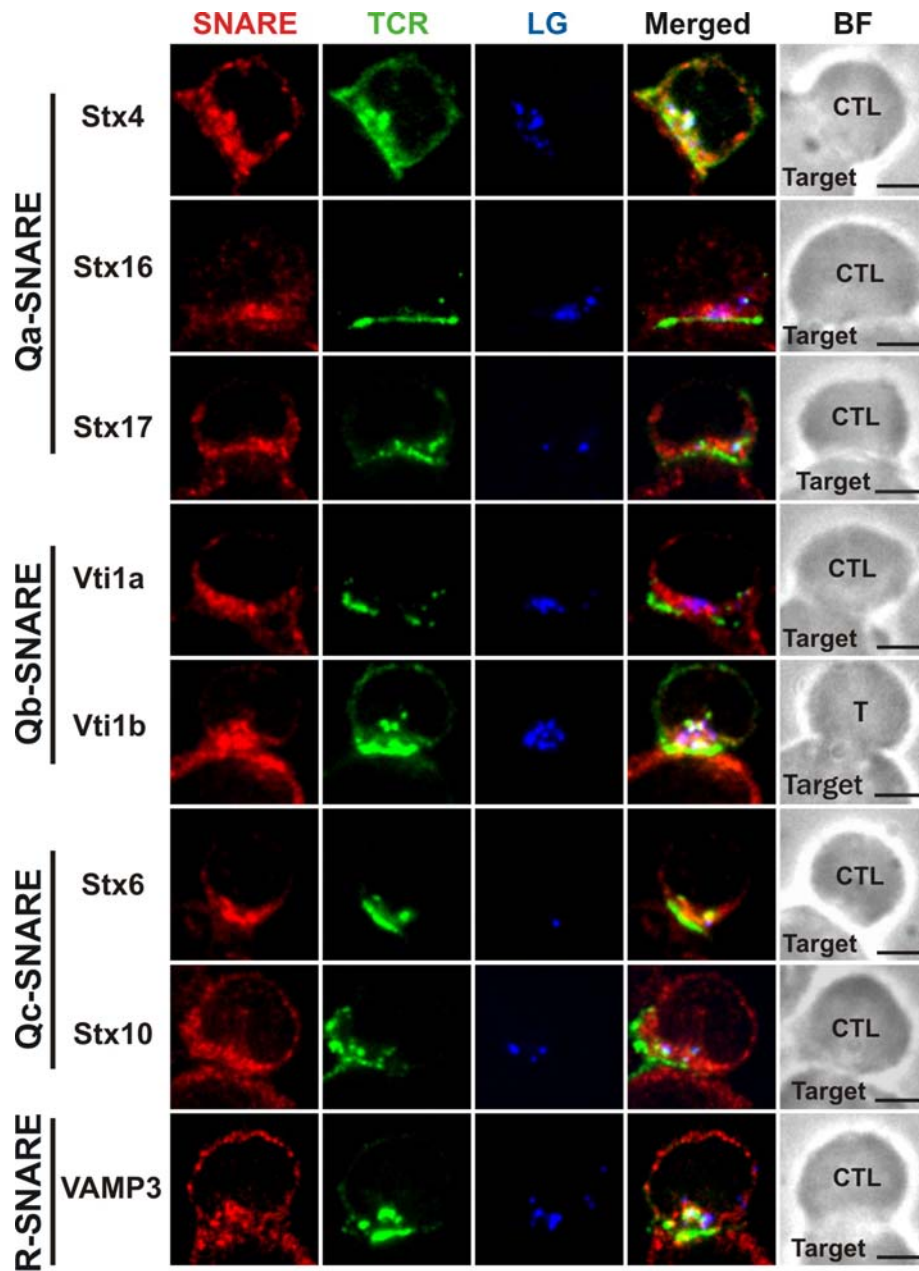


Figure 11. Localization of SNARE proteins, TCR and LG in CTLs. CTLs were incubated with SEA-pulsed Raji cells at 37 °C for 30 min and then were fixed with 4% ice-cold PFA. TCR were stained with Alexa⁴⁸⁸-conjugated anti-CD3 mAb. LG were labeled with Alexa⁶⁴⁷-conjugated anti-perforin mAb. Scale bars are 3 μ m.

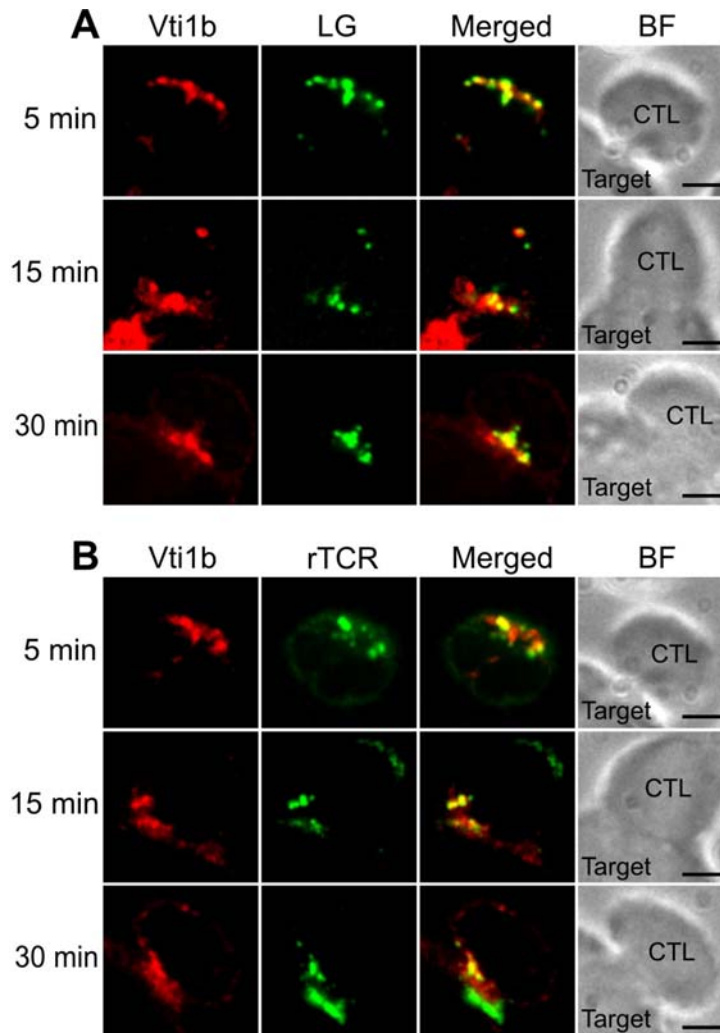


Figure 12. Vti1b co-localizes with LG as well as rTCR. CTLs were incubated with SEA-pulsed Raji cells and fixed with ice-cold 4% PFA at different time points. LG were marked with Alexa⁶⁴⁷-conjugated perforin mAb (**A**) and rTCR were labeled by pre-incubation the CTLs with Alexa⁴⁸⁸-conjugated anti-CD3 mAb (**B**). Scale bars are 3 μ m.

4.3.2 *Vti1b co-localizes with paired lytic granules*

To verify localization of Vti1b and LG/rTCR pairs, we performed a triple staining for Vti1b, recycling TCR and lytic granules in resting CTLs. We found that Vti1b co-localized

very well with LG/rTCR pairs (Fig. 13A). In order to examine the localization in a more precise manner, we circled the vesicular structure of Vti1b, recycling TCR and lytic granules, and then merged these three circles in a diagram. It showed that in many cases, Vti1b was co-localized with LG/rTCR pairs (Fig. 13B, upper panel); occasionally Vti1b was co-localized with only lytic granules or recycling TCR in the corresponding LG/rTCR pair (Fig. 13B, lower panel). Considering these data we hypothesized that Vti1b is likely to be involved in pairing of lytic granules and recycling TCR.

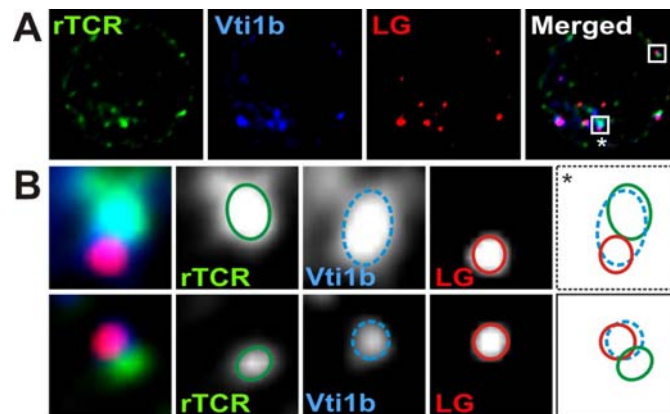


Figure 13. LG/rTCR pairs are co-localized with Vti1b. (A) Co-localization of Vti1b with LG and rTCR. CTLs were pre-incubated with Alexa⁴⁸⁸-labeled anti-CD3 mAb to label rTCR (green). Perforin was used as the LG marker (red). A polyclonal rabbit anti-Vti1b antibody was used to stain endogenous Vti1b. Two framed examples of paired vesicles were enlarged in (B), rTCR, Vti1b, LG were circled in green, blue and red, respectively. These three circles were merged in the diagram in the far right panel.

4.3.3 The possibility of vesicle pairing was enhanced by Vti1b

To determine whether Vti1b can affect LG/rTCR pairing, we analyzed the pairing possibilities under different circumstances. When lytic granules contain Vti1b, the pairing rate is three fold higher than those without Vti1b (Fig. 14). Similarly, when recycling TCR

are not co-localized with Vti1b, the possibility for pairing with lytic granules is much lower (Fig. 14). This analysis showed that Vti1b enhanced the pairing possibility for both lytic granules and recycling TCR compartments.

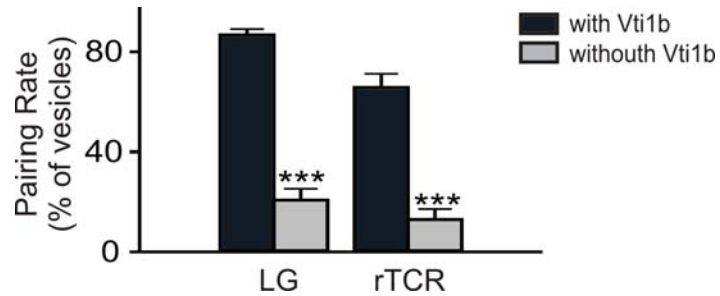


Figure 14. Vti1b increases the possibility of vesicle pairing. Vesicles co-localized with or without Vti1b are shown as black and gray bars, respectively. From left to right 285, 71, 162 and 139 vesicles in 15 cells were analyzed.

4.4 Vti1b-dependent tethering of lytic granules and recycling TCR is required for CTL cytotoxicity

4.4.1 Vti1b is required for tethering of lytic granules and recycling TCR

4.4.1.1 Vti1b expression was down-regulated efficiently by siRNA

To verify whether Vti1b is essential for the interaction between lytic granules and recycling TCR, we used RNA interference technique to down-regulate Vti1b expression. One technical difficulty is that the commonly used double-stranded siRNA are not stable enough in primary T cells. Recently, a new strategy has been designed to solve this problem. Chemical modifications (2'- deoxy-modification, 2'-methoxy-modification, 2'-hydroxyethylmethylmodification) on certain nucleotides of siRNA make the double

4. Results

strands more stable in primary T cells and this modification of siRNA can efficiently down-regulate protein expression in primary T cells¹⁷⁰. Introducing this modification into Vti1b-siRNA, we were able to efficiently down-regulate Vti1b in human primary CTLs as confirmed by quantitative RT-PCR (Figure 15A), western blot (Figure 15B) and immunocytochemistry compared to control siRNA (Figure 16A). We found that Vti1b mRNA was reduced to the lowest level between 24 to 36 hours after siRNA electroporation and then went up again (Fig. 15A). Accordingly, the protein level of Vti1b reached also the low point at 36 hr after siRNA electroporation (Fig. 15B). Therefore 36 hours after siRNA electroporation was chosen as the time point to examine the impact of Vti1b on pairing of lytic granules and recycling TCR.

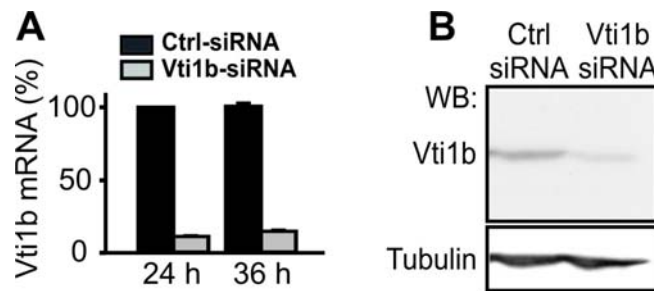


Figure 15. Down-regulation of Vti1b by modified siRNA in primary CTLs. (A) Expression of Vti1b was down-regulated by siRNA at mRNA level. 6×10^6 SEA-stimulated CTLs were electroporated with 120 pMol of control-siRNA or Vti1b-siRNA. At various time points after electroporation CTLs were harvested for qRT-PCR. The mRNA level of Vti1b was normalized with three different house-keeping genes. (B) Expression of Vti1b was down-regulated by siRNA at protein level. 36 hr after electroporation CTLs were collected in sample buffer and sonicated. One representative experiments from three independent experiments is shown.

4.4.1.2 Down-regulation of Vti1b reduced the pairing rate

The CTLs transfected with control or Vti1b-siRNA were used 36 hours after electroporation. The CTLs were first pre-incubated with Alexa⁴⁸⁸-conjugated anti-CD3 antibody to label recycling TCR, and were then fixed and stained with Alexa⁶⁴⁷-conjugated anti-perforin antibody to label the lytic granules. As shown in Fig. 16A, the pairing rate of lytic granules was reduced when Vti1b was down-regulated by modified siRNA. The quantitative analysis of Fig. 16A showed that in Vti1b-siRNA transfected CTLs the number of paired lytic granules reduced to half of the control level, whereas the number of single lytic granules increased. However, the total number of lytic granules remained unchanged.(Fig. 16B). We conclude that Vti1b is important for pairing of lytic granules and recycling TCR compartments.

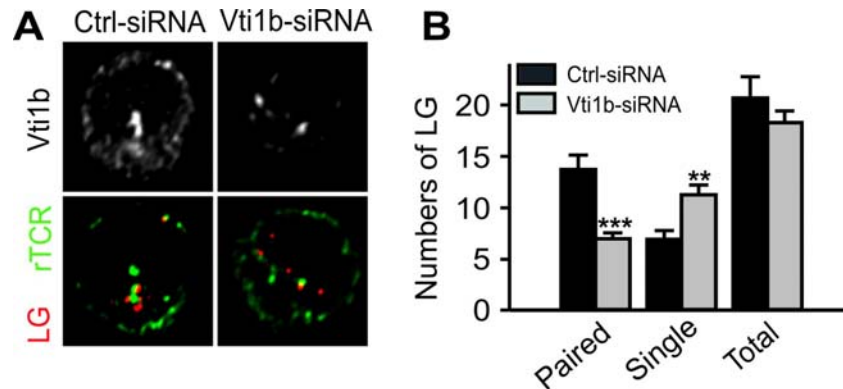


Figure 16. The pairing rate of LG was reduced by down-regulation of Vti1b. 36 hr after transfection of siRNA, CTLs were fixed and the pairing rate of LG was examined with cell observer. CTLs were pre-incubated with Alexa⁴⁸⁸-labeled anti-CD3 mAb to label rTCR. Perforin was used as the LG marker. Non-silencing siRNA was used as the control for Vti1b-siRNA. (A) Expression of Vti1b is shown in the upper panel. Pairing of LG and rTCR is shown in the lower panel. (B) Down-regulation of Vti1b reduced pairing rate of LG but not the total LG number.

4.4.2 CTL cytotoxicity is impaired by down-regulation of *Vti1b*

4.4.2.1 Accumulation of lytic granules at the IS is impaired by down-regulation of *Vti1b*

To assess whether *Vti1b*-dependent LG/rTCR pairing is necessary for lytic granules accumulation at the IS, we examined lytic granule accumulation at the IS in *Vti1b*-siRNA transfected CTLs. In *Vti1b*-siRNA transfected CTLs, lytic granules showed a scattered pattern 30 minutes after target cell contact, whereas recycling TCR were still enriched at the IS as in control siRNA transfected CTLs (Fig. 17). We conclude that down-regulation of *Vti1b* does not affect TCR recycling and reorientation towards the IS, implying that the downstream signaling and general polarization mechanisms in *Vti1b* down-regulated CTLs are still functional. Thus, the reduction of LG accumulation at the IS in *Vti1b*-siRNA treated cells is not linked to a general T cell polarization failure but rather to the specific impairment in LG/eTCR pairing.

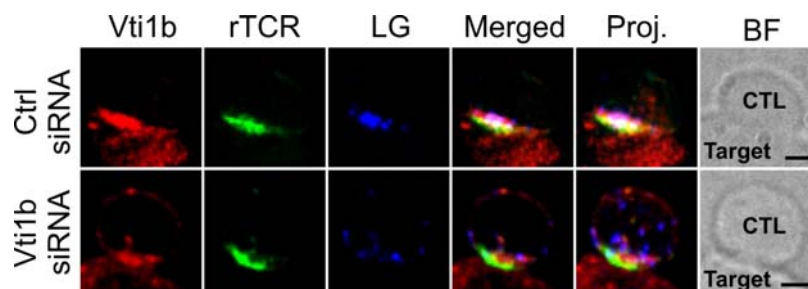


Figure 17. Down-regulation of *Vti1b* impaired the accumulation of LG at the IS. 36 hr after transfection of siRNA, CTLs were fixed and the pairing rate of lytic granules was examined with cell observer. CTLs were pre-incubated with Alexa⁴⁸⁸-labeled anti-CD3 mAb to label rTCR. Perforin was used as the lytic granule marker. Non-silencing siRNA was used as the control for *Vti1b*-siRNA. Proj., the projection of the merged stack. BF, bright field. Representative conjugates from three independent experiments are shown. Scale bars are 3 μ m.

4. Results

To quantify the reduction of lytic granule accumulation at the IS by down-regulation of Vti1b in live CTLs, we used TIRF microscopy. In agreement with the confocal microscopy results in, in Vti1b-siRNA transfected CTLs the accumulation of lytic granules was intensively inhibited, whereas in control siRNA-transfected CTLs, lytic granules showed robust accumulation at the IS (Fig. 18).

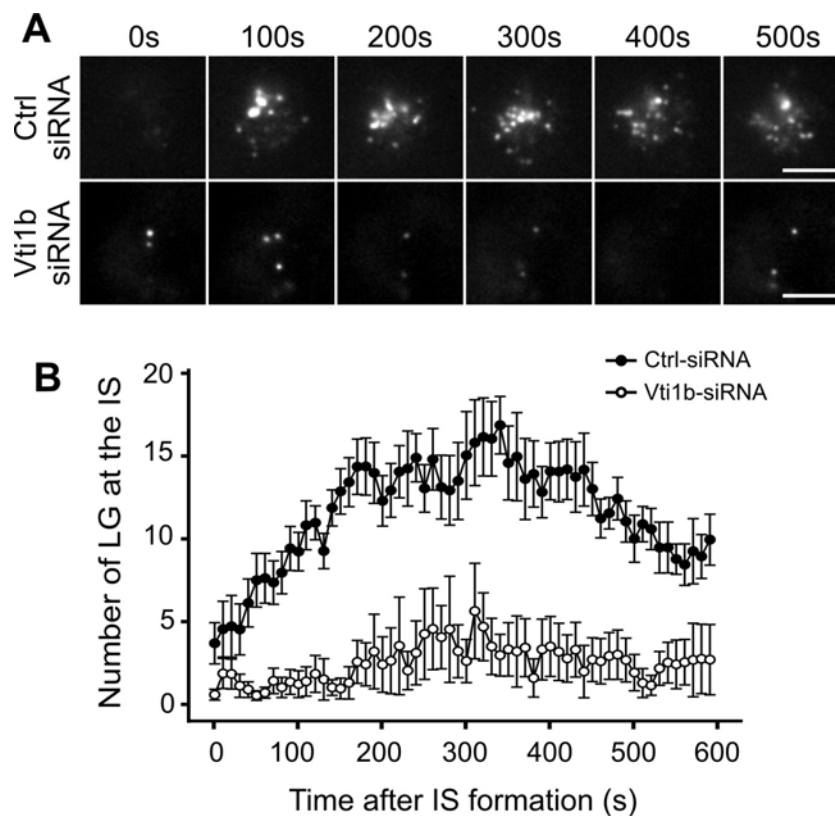


Figure 18. TIRF microscopy analysis following Vti1b down-regulation. CTLs were transfected with perforin-mCherry constructs and Vti1b-siRNA (or non-silencing control siRNA). The cells were used for TIRF microscopy 36 hours after transfection. The quantification analysis of LG accumulation is shown in **B**. The TIRF images were acquired every 1 second for 600 seconds. The numbers of lytic granules shown in the TIRF plane were quantified. Solid circles, non-silencing control siRNA; Open circles, Vti1b-siRNA. Representative examples from three independent experiments are shown. Scale bars are 3 μ m.

4.4.2.2 CTL-mediated target cell killing is impaired by down-regulation of Vti1b

We subsequently examined the CTL-mediated target cell killing in Vti1b down-regulated CTLs. The CTLs were incubated with SEA-pulsed Raji cells at various effector : target cell ratios at 37 °C for 4 hours and then the activity of lactate dehydrogenase (LDH), which is released into the supernatant by apoptotic target cells, was determined with the non-radioactive cytotoxicity assay. Consistent with impaired lytic granule accumulation at the IS, the killing capacity of Vti1b siRNA-transfected CTLs showed a significant reduction (Fig. 19). Together with the results above, we demonstrate that Vti1b is essential for LG/rTCR pairing and is subsequently of great importance for CTL-mediated cytotoxicity.

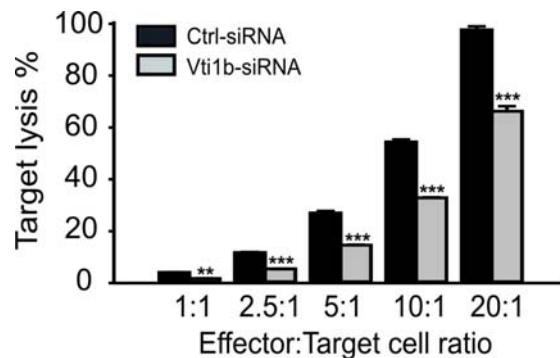


Figure 19. Down-regulation of vti1b impaired CTL cytotoxicity. 36 hr after electroporation CTLs were incubated with SEA-pulsed Raji cells at 37 °C for 4 hr with various ratios. Then the supernatant was collected for the NonRadioactive cytotoxicity assay. One representative example from three independent experiments is shown.

4.5 Vti1b may co-operate with AP-3 to mediate tethering

Since Vti1b can bind with the epsin receptor¹⁷⁷⁻¹⁷⁸, an adaptor protein in the Golgi apparatus. It is possible that lytic granules and recycling TCR compartments may be tethered by the interaction between Vti1b and an adaptor protein. Considering the known

4. Results

immune disorders in humans, only the Hermansky-Pudlak syndrome 2 (HPS2), caused by deficiency in AP-3¹⁵⁴, has been characterized to be defective in lytic granule accumulation at the IS. Lack of AP-3 leads to a scattered pattern of lytic granules in CTLs even after IS formation¹⁵⁴, which is similar to our findings in Vti1b down-regulated CTLs (Fig. 17 and Fig. 18). Interestingly, similar to Vti1b, AP-3 was not only re-positioned at the IS during IS formation, but also co-localized with recycling TCR as well as lytic granules (Fig. 20 A and B). Given the fact that AP-3 was also co-localized with Vti1b (Fig. 20C), we propose that vti1b and AP-3 could cooperate to regulate LG/rTCR pairing and thus regulate lytic granule accumulation and release at the IS.

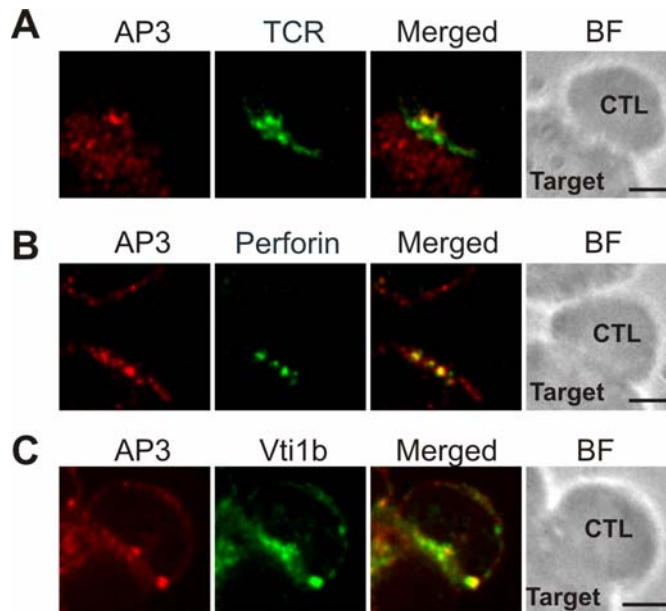


Figure 20. Localization of AP-3 in CTLs. AP-3 was co-localized with TCR (A), lytic granules (B) and Vti1b (C). SEA-specific CTLs were incubated with SEA-pulsed Raji cells for 15 min and then the samples were fixed with ice-cold 4% PFA. Scale bars are 3 μ m.

4.6 Model for paired vesicle transport

Our results show that lytic granules and rTCR can be co-transported to the IS. The interaction of lytic granules with rTCR is necessary for their efficient docking and release at the IS. An important parameter of the immune response is the speed of target cell killing by CTLs because it determines the efficiency of cell killing. Using data sets acquired with confocal microscopy (as shown in Fig. 2A), we modeled vesicle transport using a compartment model as sketched in Fig. 21A and formulated the dynamic changes in the various vesicle pools mathematically (Fig. 21B). The rate constants obtained from the model (Fig. 21C) predict the numbers of paired and single lytic granules in different areas of the cell (for instance in proximity of the IS) over time (solid lines in Fig. 22). These predictions are in good agreement with the experimental data (squares and circles in Fig. 22) indicating that the model is appropriate to fit the data. The model could only fit the data well in case the transport rates k_1 to k_6 were changed between 5 and 10 minutes after target cell recognition. The model also shows that 10 minutes after target cell contact the LG/rTCR pairing rate k_2 increases by a factor of four compared to the early IS formation phase, i.e. the first 5 minutes after IS formation; and also k_3 , the rate of transport paired lytic granules to the IS, increases by a factor of four. In contrast, the rates k_4 and k_5 for transport of single lytic granules towards and away from IS, respectively, remained unchanged. The model also predicts that 10 minutes after target cell contact, more new lytic granules are generated since k_1 is increased. Up-to-date imaging approaches, without modifying the endogenous proteins, still cannot measure the lytic granule generation *in vivo*. Our model reveals for the first time that after CTLs form a contact with target cells, new lytic granules are generated ($k_1 > 0$) to refill the cytotoxic granule pool and compensate for the released lytic granules.

4. Results

Finally the model shows that lytic granules can be released even at the early stage of IS formation since $k_6 = 0.25 \text{ min}^{-1}$ and more than four paired vesicles at the IS imply the release of at least one lytic granule per minute. Thus our data and model predict that CTLs can kill with a high efficiency within a few minutes using the pairing mechanism because it guarantees the rapid and efficient accumulation of lytic granules at the IS.

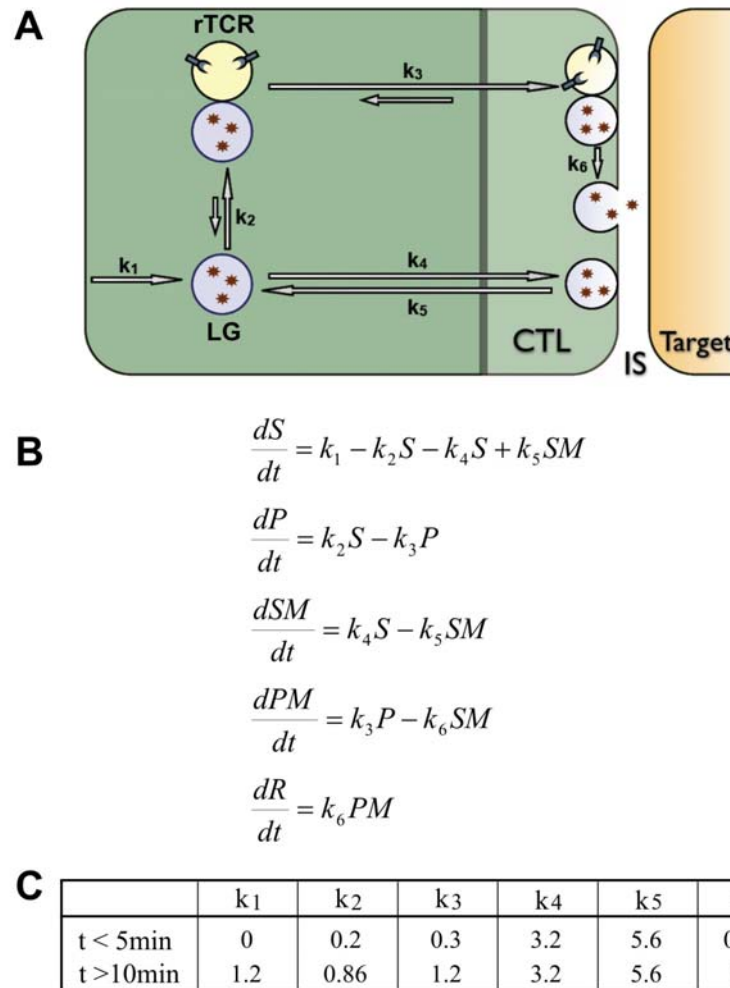


Figure 21. Model for paired vesicle transport. (A) Paired and single lytic granule transport. Pairing is required for lytic granule enrichment at the IS and to facilitate their release. k_1 is the rate of perforin granule production. k_2 is the rate of formation of paired vesicles. k_3 , the rate of movement of paired vesicles to the area in the proximity of the IS. k_4 is the rate of single vesicles moving to the area in the proximity of the IS; k_5 is the reverse rate of k_4 . k_6 is the rate of paired vesicle release. (B) The formulas to describe changes in the different vesicle pools. SM, the single lytic granules in proximity to the IS; PM, the paired lytic granules in proximity to the IS; S, the single lytic granules far from the IS (not in proximity to the IS); P, the paired lytic granules far from the IS. (C) The parameters used for the compartment model.

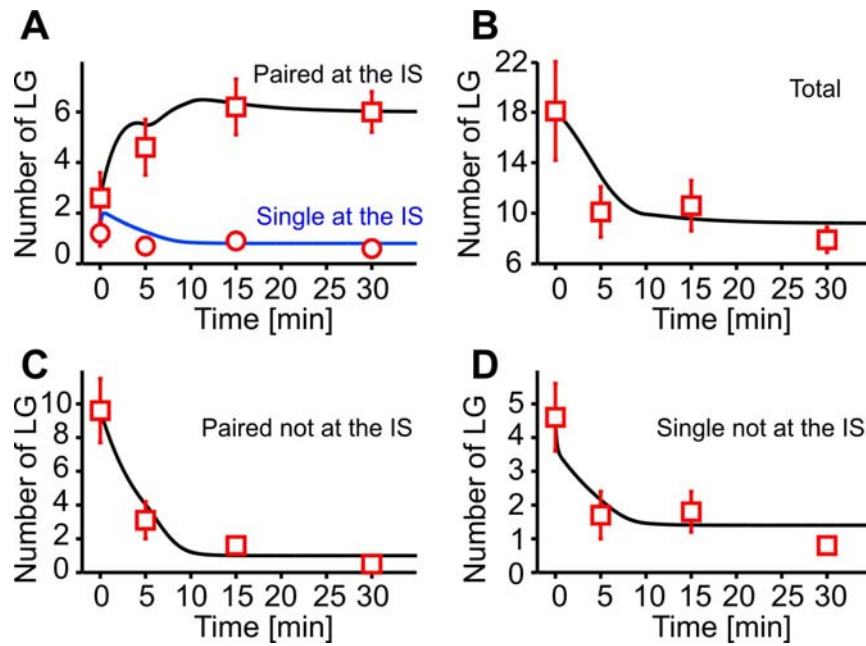


Figure 22. Paired LG transport model fits the experimental results. CTLs were incubated with SEA-pulse Raji cells and fixed at 5, 15 and 30 min. Resting CTLs were taken as 0 min. Dots (or squares) are the experimental results. Lines are the predicted curves from the model. **(A)** Upon increasing time, the number of paired LG (squares) at the IS was increasing while the number of single LG (dots) at the IS remained almost unchanged. **(B)** Over time the total number of LG was decreased. The number of both paired **(C)** and single **(D)** LG not at the IS was decreased.

5. Discussion

This study establishes Vti1b as a mediator for the interaction between lytic granules and recycling TCR compartments. A close interaction between lytic granules and recycling TCR compartments is required for the accumulation and secretion of lytic granules at the IS. Vti1b down-regulation by RNA interference decreased the probability of the interaction between lytic granules and recycling TCR compartments, resulting in an impairment in accumulation and release of lytic granules at the IS and a reduction in CTL-mediated cytotoxicity.

5.1 Significance of tethering of two organelles

5.1.1 *En passant killing*

A very important parameter of the immune response is the speed of target cell killing by CTLs because it may determine the outcome of an immune response. Using data from confocal experiments that were performed at 37 °C at various time points after contact (as shown in Figure 2A), our model predicts that 5 minutes after IS formation the transport rate constants are accelerated and that the rate of lytic granule production is increased to 1 granule per minute. Furthermore, the number of released vesicles increases at a rate of about 1 granule per minute immediately after IS formation. We conclude that CTLs need only a few minutes to secrete lytic granules at the IS, supporting an *en passant* killing process.

In line with this prediction, Purbhoo et al.¹⁷⁹ have shown that a mature immunological synapse is not required for cytotoxicity. They found that CTLs were able to detect a single

5. Discussion

foreign antigen, three antigen-MHC complexes were necessary for killing but ten were needed for full signaling including a sustained Ca^{2+} increase. These findings are not easy to reconcile with the finding that a full polarization of CTLs, including MTOC translocation to the IS, is required for CTLs cytotoxicity¹³⁶ because the full polarization of CTLs certainly involves sustained signaling. Stinchcome *et al.* observed a very close apposition of MTOC and IS highlighting the role of the MTOC for lytic granule delivery and exocytosis. This intimate MTOC-IS contact was observed in 17% of activated CTLs¹³⁶.

Considering our new findings and the compartment model, we suggest a hypothetical model to reconcile the data by Purbhoo *et al.*¹⁷⁹ and Stinchcome *et al.*¹³⁶: MTOC translocation, which is induced by a strong interaction between CTLs and target cells, can guarantee killing but at the cost of time; LG/rTCR tethering-mediated reorientation and secretion of lytic granules at the IS enables CTLs to kill more target cells (maybe even in parallel) in a shorter time, but with the risk of having a failed killing occasionally. The stronger the interaction between CTLs and target cells, the more likely it is that the MTOC translocates to the IS leading to the accumulation of all lytic granules at the IS¹³⁶, ensuring the elimination of the target cells. However, the weak interaction between CTLs and target cells, which occurs with less than 10 antigen-MHC complexes, is not able to provide strong sustained signaling required for MTOC translocation¹⁷⁹. Nevertheless, transport and docking of lytic granules at the IS can still be achieved rapidly by the Vti1b-dependent interaction between lytic granules and rTCR. Breaking up of synapses before IS maturation and full polarization of CTLs¹⁸⁰⁻¹⁸² can also help CTLs to save time and significantly speed up killing. Under physiological circumstances, target cells with high virus load (corresponding to the strong CTL-target cell interaction) should be destroyed with a very high reliability, which can be assured by full polarization of the killing machinery

involving MTOC translocation. On the other hand, for target cells with a relatively low virus load (corresponding to the weak CTL-target cell interaction) a rapid killing mechanism with a potentially slightly lower reliability may be advantageous. Indeed it has been reported that, at low doses of antigen, MTOC reorientation to the IS was decreased¹⁸³. In this case, the Vti1b-dependent interaction between lytic granules and rTCR provides another mechanism to kill these target cells without MTOC reorientation.

5.1.2 Balance between TCR function and TCR down-regulation

TCR/CD3 complexes are constantly internalized and recycled back to the cell surface. TCR recycling has been shown to be crucial for IS formation¹⁸⁴. To fulfill the task to eliminate target cells, it is important for CTLs to maintain sensitivity to antigens, which requires a certain expression level of TCR/CD3 complexes in CTLs. To detach from killed target cells or to refill the exhausted cytotoxic granule pool, CTLs need to down-tune their ability to engage with target cells by down-modulating TCR/CD3 expression. It has been reported that TCR/CD3 complexes can be targeted to lysosomes by a di-leucine motif¹⁸⁵ and can be down-regulated after 1 hour of TCR engagement¹⁸⁶. To balance between maintenance of functional TCR and antigen-induced TCR down-regulation is a big challenge for CTLs.

Tethering of lytic granules and recycling TCR compartments may be a good solution for this problem. By tethering with lytic granules, recycling TCR compartments can quickly facilitate the accumulation and release of lytic granules at the IS without being degraded in lytic granules. On the other hand, the closer to the IS, the higher calcium influx would be, which means that the longer LG/rTCR pairs stay in vicinity of the IS, the higher is the

chance they would be exposed to high concentration of calcium. As a result, some time after target cell recognition, tethered lytic granules and TCR compartments can fuse after which TCR are consequently down-regulated. But it is likely for the fusion of LG/rTCR to occur only at the late stage of CTL-target cell engagement. It assures TCR down-regulation without jeopardizing initial killing capacity of CTLs.

5.1.3 General signaling mechanism

The concept of organelle tethering has recently gained much attention, since de Brito and Scorrano have shown that mitofusin 2 tethers ER to mitochondria, which facilitates efficient mitochondrial Ca^{2+} uptake ¹⁸⁷. In macrophages, a tethering-like structure of recycling transferrin receptors and IL-6 containing secretory granules has also been shown ¹⁸⁸. We screened the literature for images of other potentially tethered organelles and found hints for paired vesicles also in other cell types, such as mouse embryonic fibroblasts and NRK fibroblast cells ¹⁸⁹⁻¹⁹⁰. Interaction of different vesicles is usually thought to be a transition state right before vesicle fusion. But co-localization of lytic granules and recycling TCR compartments was observed only in very few cases in our results, indicating that fusion is not necessarily the destined fate for two tethered compartments, in other words, rather than just a transit state, interaction of different vesicles can stay as a stable structure to fulfill their functions, such as transporting or relocating vesicles.

Menager *et al.* reported that cytotoxic function of CTLs required the Munc13-4 mediated cooperation of cytotoxic granules and Rab11-positive endosomal ‘exocytic vesicles’ ¹⁹¹. Their work highlights the Rab11-mediated recycling pathway for the maturation of cytotoxic granules. Our work further verifies that regulatory recycling endosomes — in

particular, TCR-containing recycling endosomes — play a pivotal role in lytic granule release at the IS by tethering with lytic granules and stabilizing them at the IS, thereby enhancing the lytic granule release probability. In Munc13-4 deficient CTLs, it is shown that lytic granules are still reoriented to the IS but cannot be released¹⁹¹. In Vti1b-downregulated CTLs, lytic granules cannot accumulate at the IS because of the impairment in tethering with rTCR. These findings suggest that the Vti1b-mediated interaction between lytic granules and rTCR compartments is located upstream of Munc13-4 regulated cooperation of LG and exocytotic vesicles.

5.2 How Vti1b mediates tethering

The exact role of Vti1b in vesicle pairing has yet to be elucidated and further studies are required to establish its various functions in primary T-cells. However, both in Vti1b down-regulated CTLs (Fig. 17 and Fig. 18) and in AP-3 deficient CTLs¹⁵⁴, the re-orientation of lytic granules at the IS is defective. Furthermore AP-3 and Vti1b are colocalized in CTLs and AP-3 is localized with TCR compartments and lytic granules in a similar manner as Vti1b (Fig. 20). This data implies that Vti1b may co-operate with AP-3 to mediate LG/rTCR tethering and thus regulate CTL function. In addition, there are at least two other possibilities for Vti1b to regulate pairing. First, it has been reported that Vti1b can form oligomers in vitro¹⁹². Vti1b therefore appears to have the capability to tether two juxtaposed compartments by homo-interaction. Second, Vti1b can form a trans-SNARE complex with its cognate SNARE proteins — syntaxin 7, syntaxin 8, VAMP7 or VAMP8¹³⁸, which may tether lytic granules and recycling TCR compartments under the circumstances inappropriate for vesicle fusion.

5.3 What does the model tell us

Lytic granules are the main weapon that CTLs rely on to eliminate target cells. But many questions, such as how quickly CTLs release lytic granules after target cell recognition, whether new lytic granules are generated during killing or after killing, are yet to be answered. In our study, a compartment model was formulated in the basis of experimental data acquired with confocal microscopy. The model predicted that lytic granules are released at a rate of 1 lytic granule per minute after contact formation between CTLs and the target cells, moreover new lytic granules started to be generated 10 minutes after IS formation at a rate of 1.2 granules per minute. It's the first time to show the dynamic information of endogenous lytic granules *in vivo*. Our results provide an explanation for fast CTL killing in a quantitative way. Furthermore, our finding that new lytic granules are generated during the killing provides an insight about how CTLs maintain killing capacity to eliminate several target cells.

More importantly, our model revealed that after IS formation, transport of paired lytic granules to the IS was accelerated, in contrast, there was not much change in the dynamics of single lytic granules. This result further elucidates the functional importance of tethering between lytic granules and recycling TCR compartments. The increase in the transport rate of LG/rTCR pairs could be contributed by the longer dwell times of paired lytic granules at the IS and/or the reorientation of the whole secretory machinery, including MTOC relocalization. MTOC relocalization is an energy-consuming process, normally it takes more than 15 minutes^{105,136}. Therefore, the increase in the transport rate of paired lytic granules at the early stage of IS formation — within 15 minutes after target cell recognition — is likely mediated by longer dwell times of paired lytic granules at the IS.

5.4 Why the Golgi apparatus is reoriented to the IS

Golgi apparatus reorientation to the T cell-target cell interface is one of the first hallmarks identified to be required for CTL-mediated killing^{115,193}. As the Golgi apparatus is the main hub for recycling pathways as well as for modifying, sorting and packaging proteins for secretion, it is reasonable to assume that reorientation of the Golgi apparatus to the IS is to build a shortcut to facilitate delivery of newly generated lytic granules to the IS. But until now, not many studies have been done to verify the functions of the Golgi apparatus at the IS. Our compartment model suggests that new lytic granules are generated immediately after IS formation to refill the cytotoxic granule pool. Very recently Makedonas *et al.* has also shown that newly synthesized perforin rapidly appears at the IS, both in association with and independent of cytotoxic granules¹⁹⁴, which is a strong support of our prediction.

Our data show that some LG/rTCR pairs were colocalized with the Golgi apparatus and disassembly of Golgi apparatus led to a complete loss of lytic granule accumulation at the IS (Fig. 10). This indicates that the Golgi apparatus could be the place for assembly of LG/rTCR pairs and that it plays a crucial role in controlling transport of LG/rTCR pairs. Potentially the Golgi apparatus generates new lytic granules and then tethers them with recycling TCR compartments. Thus, closer the Golgi apparatus is to the IS, lesser is the time lytic granules would need to approach the IS and the target cells could be eliminated faster. Combining the above two points, we propose that reorientation of the Golgi apparatus to the IS enhances the efficiency of CTL-mediated killing.

5.5 Error estimation

5.5.1 *The fate of tethered recycling TCR compartments*

In the CTLs recorded with fast 4D microscopy, we never found any separation of the paired LG/rTCR. One technical problem we encountered was that the fluorophore Alexa⁴⁸⁸ conjugated to anti-CD3 antibody was bleaching relatively quickly with time. To minimize the interference caused by bleaching, we recorded the cells only in the first 10 to 15 minutes after IS formation. Therefore we can not rule out the possibility that detaching of paired lytic granules and recycling TCR compartments could occur at a relatively late stage of IS formation.

Our data show that recycling TCR facilitate lytic granule docking at the plasma membrane and as a consequence, paired lytic granules are released more frequently at the IS than single lytic granules (Fig. 8 and related text). After the lytic granules are released, what is the fate of cognate paired recycling TCR compartments? Are they fused with the plasma membrane or do they stay docked at the plasma membrane or simply go back to the cytosol? From our results acquired by TIRF microscopy, we found that after paired lytic granule secretion, the cognate recycling TCR compartment always stayed at the TIRF plane for some time. Limited by the resolution of TIRF microscopy, we are not able to distinguish the recycling TCR compartments docked at the plasma membrane from the TCR microclusters incorporated into the plasma membrane. In addition, the fluorophore Alexa⁴⁸⁸, which is conjugated with the antibody against CD3, is bleached with time during recording. Therefore when an Alexa⁴⁸⁸-conjugated anti-CD3 antibody labeled TCR compartment vanishes, it is difficult to judge whether it has fused with the plasma membrane or the labeling fluorophore Alexa⁴⁸⁸ is bleached. Restrained by the technique

limitations, the fate of recycling TCR compartments after release of cognate paired lytic granules still remains as a question to be further investigated.

5.5.2 *Two compartments or two sub-compartments*

In this study, we have resolved that lytic granules and recycling TCR compartments are tethered. Whether lytic granules and recycling TCR compartments are localized in two different compartments that are tethered together or they are contained in different “sub-compartments” of a larger organelle cannot be resolved by fluorescence microscopy. Interestingly, Peters *et al.* already showed 20 years ago that endocytosed TCR can be associated with the membranes of LG localized in lysosomes, but in a structure distinct from the dense core of the lysosomes¹⁹⁵, which most likely contains perforin. This suggests that TCR can be sorted into the lytic granule but is in a subcompartment distinct from cytotoxic proteins, such as perforin. While we did not find other evidence of a distinct localization of perforin and TCR in subcompartments of a common lytic compartment, but our data obtained from confocal microscopy, fast deconvolution microscopy, and TIRF microscopy can, at present, not rule out this possibility. At this point, we cannot distinguish between different subcompartments in one lytic granule or tethering of two different organelles. It is however obvious that perforin and rTCR do not co-localize.

5.5.3 *Secretory domain vs. multifocal IS in human CTLs*

Griffiths and coworkers have reported that in mouse CTLs signaling molecules and lytic granules were accumulated at the IS in two spacially separated domains¹⁹. The distinct

secretory domain has been thought to be one prominent feature of CTL-formed IS. We did not find the same feature in the IS formed by human CTLs using TIRF microscopy and confocal microscopy. In human CTLs, lytic granules accumulate at the IS, but not in a distinct domain separated from TCR (see Fig. 1 and Fig. 6), which is the marker for cSMAC. The most simple explanation for the discrepancy is that arrangement of the IS in human CTLs is different from mouse CTLs. Another possibility is that the status of CTL-target cell engagement was not the same in two studies. In Griffiths' work, the mouse CTLs were incubated with target cells for 40 to 60 minutes before fixation, however, we incubated human CTLs with target cells for only 5 to 30 minutes before fixation. In other words, the distinct secretory domain at the IS could also be a feature for late stage of CTL-target cell engagement, which is not shown in the early stage of CTL-target cell engagement. We have demonstrated in our study that CTLs can release lytic granules quickly, within 5 minutes after target cell recognition (see Fig. 22). Therefore it is unlikely that a distinct secretory domain is necessary for lytic granule release.

6. References

1. Pancer, Z. & Cooper, M. D. The evolution of adaptive immunity. *Annu Rev Immunol* **24**, 497-518 (2006).
2. Flajnik, M. F. & Du Pasquier, L. Evolution of innate and adaptive immunity: can we draw a line? *Trends Immunol* **25**, 640-4 (2004).
3. Cannon, J. P., Haire, R. N., Rast, J. P. & Litman, G. W. The phylogenetic origins of the antigen-binding receptors and somatic diversification mechanisms. *Immunol Rev* **200**, 12-22 (2004).
4. Eason, D. D. et al. Mechanisms of antigen receptor evolution. *Semin Immunol* **16**, 215-26 (2004).
5. Wagle, N. M. et al. B-lymphocyte signaling receptors and the control of class-II antigen processing. *Curr Top Microbiol Immunol* **245**, 101-26 (2000).
6. Kehry, M. R. & Hodgkin, P. D. B-cell activation by helper T-cell membranes. *Crit Rev Immunol* **14**, 221-38 (1994).
7. Castellino, F. & Germain, R. N. Cooperation between CD4+ and CD8+ T cells: when, where, and how. *Annu Rev Immunol* **24**, 519-40 (2006).
8. Abbas, A. K., Murphy, K. M. & Sher, A. Functional diversity of helper T lymphocytes. *Nature* **383**, 787-93 (1996).
9. Stinchcombe, J. C. & Griffiths, G. M. Secretory mechanisms in cell-mediated cytotoxicity. *Annu Rev Cell Dev Biol* **23**, 495-517 (2007).

6. References

10. Kaech, S. M., Wherry, E. J. & Ahmed, R. Effector and memory T-cell differentiation: implications for vaccine development. *Nat Rev Immunol* **2**, 251-62 (2002).
11. Kos, F. J. & Engleman, E. G. Immune regulation: a critical link between NK cells and CTLs. *Immunol Today* **17**, 174-6 (1996).
12. Butcher, E. C. & Picker, L. J. Lymphocyte homing and homeostasis. *Science* **272**, 60-6 (1996).
13. Carbone, F. R., Kurts, C., Bennett, S. R., Miller, J. F. & Heath, W. R. Cross-presentation: a general mechanism for CTL immunity and tolerance. *Immunol Today* **19**, 368-73 (1998).
14. Harding, F. A. & Allison, J. P. CD28-B7 interactions allow the induction of CD8+ cytotoxic T lymphocytes in the absence of exogenous help. *J Exp Med* **177**, 1791-6 (1993).
15. Allison, J. P. CD28-B7 interactions in T-cell activation. *Curr Opin Immunol* **6**, 414-9 (1994).
16. Zagury, D. Direct analysis of individual killer T cells: susceptibility of target cells to lysis and secretion of hydrolytic enzymes by CTL. *Adv Exp Med Biol* **146**, 149-69 (1982).
17. Yannelli, J. R., Sullivan, J. A., Mandell, G. L. & Engelhard, V. H. Reorientation and fusion of cytotoxic T lymphocyte granules after interaction with target cells as determined by high resolution cinemicrography. *J Immunol* **136**, 377-82 (1986).
18. Peters, P. J. et al. Cytotoxic T lymphocyte granules are secretory lysosomes, containing both perforin and granzymes. *J Exp Med* **173**, 1099-109 (1991).

6. References

19. Stinchcombe, J. C., Bossi, G., Booth, S. & Griffiths, G. M. The immunological synapse of CTL contains a secretory domain and membrane bridges. *Immunity* **15**, 751-61 (2001).
20. Lyubchenko, T. A., Wurth, G. A. & Zweifach, A. Role of calcium influx in cytotoxic T lymphocyte lytic granule exocytosis during target cell killing. *Immunity* **15**, 847-59 (2001).
21. Barry, M. & Bleackley, R. C. Cytotoxic T lymphocytes: all roads lead to death. *Nat Rev Immunol* **2**, 401-9 (2002).
22. Rouvier, E., Luciani, M. F. & Golstein, P. Fas involvement in Ca(2+)-independent T cell-mediated cytotoxicity. *J Exp Med* **177**, 195-200 (1993).
23. Kreuwel, H. T. et al. Comparing the relative role of perforin/granzyme versus Fas/Fas ligand cytotoxic pathways in CD8+ T cell-mediated insulin-dependent diabetes mellitus. *J Immunol* **163**, 4335-41 (1999).
24. Strasser, A., Jost, P. J. & Nagata, S. The many roles of FAS receptor signaling in the immune system. *Immunity* **30**, 180-92 (2009).
25. Ausiello, C., Sorrentino, V., Ruggiero, V. & Rossi, G. B. Action of lysosomotropic amines on spontaneous and interferon enhanced NK and CTL cytolysis. *Immunol Lett* **8**, 11-5 (1984).
26. Wang, J., Stohlman, S. A. & Dennert, G. TCR cross-linking induces CTL death via internal action of TNF. *J Immunol* **152**, 3824-32 (1994).
27. Liu, C. C., Perussia, B., Cohn, Z. A. & Young, J. D. Identification and characterization of a pore-forming protein of human peripheral blood natural killer cells. *J Exp Med* **164**, 2061-76 (1986).

6. References

28. Podack, E. R., Young, J. D. & Cohn, Z. A. Isolation and biochemical and functional characterization of perforin 1 from cytolytic T-cell granules. *Proc Natl Acad Sci U S A* **82**, 8629-33 (1985).
29. Masson, D. & Tschopp, J. Isolation of a lytic, pore-forming protein (perforin) from cytolytic T-lymphocytes. *J Biol Chem* **260**, 9069-72 (1985).
30. Trapani, J. A. Dual mechanisms of apoptosis induction by cytotoxic lymphocytes. *Int Rev Cytol* **182**, 111-92 (1998).
31. Voskoboinik, I. et al. Calcium-dependent plasma membrane binding and cell lysis by perforin are mediated through its C2 domain: A critical role for aspartate residues 429, 435, 483, and 485 but not 491. *J Biol Chem* **280**, 8426-34 (2005).
32. Uellner, R. et al. Perforin is activated by a proteolytic cleavage during biosynthesis which reveals a phospholipid-binding C2 domain. *Embo J* **16**, 7287-96 (1997).
33. Voskoboinik, I. & Trapani, J. A. Addressing the mysteries of perforin function. *Immunol Cell Biol* **84**, 66-71 (2006).
34. Clark, W. R. Immunology. The hole truth about perforin. *Nature* **369**, 16-7 (1994).
35. Kagi, D. & Hengartner, H. Different roles for cytotoxic T cells in the control of infections with cytopathic versus noncytopathic viruses. *Curr Opin Immunol* **8**, 472-7 (1996).
36. Kagi, D. et al. Cytotoxicity mediated by T cells and natural killer cells is greatly impaired in perforin-deficient mice. *Nature* **369**, 31-7 (1994).
37. van den Broek, M. E. et al. Decreased tumor surveillance in perforin-deficient mice. *J Exp Med* **184**, 1781-90 (1996).

6. References

38. Walsh, C. M. et al. Immune function in mice lacking the perforin gene. *Proc Natl Acad Sci U S A* **91**, 10854-8 (1994).
39. Smyth, M. J. et al. Perforin-mediated cytotoxicity is critical for surveillance of spontaneous lymphoma. *J Exp Med* **192**, 755-60 (2000).
40. Matloubian, M. et al. A role for perforin in downregulating T-cell responses during chronic viral infection. *J Virol* **73**, 2527-36 (1999).
41. Spaner, D., Raju, K., Rabinovich, B. & Miller, R. G. A role for perforin in activation-induced T cell death in vivo: increased expansion of allogeneic perforin-deficient T cells in SCID mice. *J Immunol* **162**, 1192-9 (1999).
42. Rosen, D. et al. Tumor immunity in perforin-deficient mice: a role for CD95 (Fas/APO-1). *J Immunol* **164**, 3229-35 (2000).
43. Chia, J. et al. Temperature sensitivity of human perforin mutants unmasks subtotal loss of cytotoxicity, delayed FHL, and a predisposition to cancer. *Proc Natl Acad Sci U S A* **106**, 9809-14 (2009).
44. Stepp, S. E. et al. Perforin gene defects in familial hemophagocytic lymphohistiocytosis. *Science* **286**, 1957-9 (1999).
45. Lieberman, J. The ABCs of granule-mediated cytotoxicity: new weapons in the arsenal. *Nat Rev Immunol* **3**, 361-70 (2003).
46. Beresford, P. J., Xia, Z., Greenberg, A. H. & Lieberman, J. Granzyme A loading induces rapid cytolysis and a novel form of DNA damage independently of caspase activation. *Immunity* **10**, 585-94 (1999).

6. References

47. Shresta, S., Graubert, T. A., Thomas, D. A., Raptis, S. Z. & Ley, T. J. Granzyme A initiates an alternative pathway for granule-mediated apoptosis. *Immunity* **10**, 595-605 (1999).
48. Chowdhury, D. & Lieberman, J. Death by a thousand cuts: granzyme pathways of programmed cell death. *Annu Rev Immunol* **26**, 389-420 (2008).
49. Shi, L., Kraut, R. P., Aebersold, R. & Greenberg, A. H. A natural killer cell granule protein that induces DNA fragmentation and apoptosis. *J Exp Med* **175**, 553-66 (1992).
50. Shi, L., Kam, C. M., Powers, J. C., Aebersold, R. & Greenberg, A. H. Purification of three cytotoxic lymphocyte granule serine proteases that induce apoptosis through distinct substrate and target cell interactions. *J Exp Med* **176**, 1521-9 (1992).
51. Martinvalet, D., Zhu, P. & Lieberman, J. Granzyme A induces caspase-independent mitochondrial damage, a required first step for apoptosis. *Immunity* **22**, 355-70 (2005).
52. Lord, S. J., Rajotte, R. V., Korbitt, G. S. & Bleackley, R. C. Granzyme B: a natural born killer. *Immunol Rev* **193**, 31-8 (2003).
53. Trapani, J. A. & Sutton, V. R. Granzyme B: pro-apoptotic, antiviral and antitumor functions. *Curr Opin Immunol* **15**, 533-43 (2003).
54. Darmon, A. J., Nicholson, D. W. & Bleackley, R. C. Activation of the apoptotic protease CPP32 by cytotoxic T-cell-derived granzyme B. *Nature* **377**, 446-8 (1995).
55. Adrain, C., Murphy, B. M. & Martin, S. J. Molecular ordering of the caspase activation cascade initiated by the cytotoxic T lymphocyte/natural killer (CTL/NK) protease granzyme B. *J Biol Chem* **280**, 4663-73 (2005).

6. References

56. Froelich, C. J. et al. Granzyme B/perforin-mediated apoptosis of Jurkat cells results in cleavage of poly(ADP-ribose) polymerase to the 89-kDa apoptotic fragment and less abundant 64-kDa fragment. *Biochem Biophys Res Commun* **227**, 658-65 (1996).
57. Andrade, F. et al. Granzyme B directly and efficiently cleaves several downstream caspase substrates: implications for CTL-induced apoptosis. *Immunity* **8**, 451-60 (1998).
58. Zhang, D., Beresford, P. J., Greenberg, A. H. & Lieberman, J. Granzymes A and B directly cleave lamins and disrupt the nuclear lamina during granule-mediated cytolysis. *Proc Natl Acad Sci U S A* **98**, 5746-51 (2001).
59. Thomas, D. A., Du, C., Xu, M., Wang, X. & Ley, T. J. DFF45/ICAD can be directly processed by granzyme B during the induction of apoptosis. *Immunity* **12**, 621-32 (2000).
60. Trapani, J. A. et al. Efficient nuclear targeting of granzyme B and the nuclear consequences of apoptosis induced by granzyme B and perforin are caspase-dependent, but cell death is caspase-independent. *J Biol Chem* **273**, 27934-8 (1998).
61. Sarin, A. et al. Target cell lysis by CTL granule exocytosis is independent of ICE/Ced-3 family proteases. *Immunity* **6**, 209-15 (1997).
62. Barry, M. et al. Granzyme B short-circuits the need for caspase 8 activity during granule-mediated cytotoxic T-lymphocyte killing by directly cleaving Bid. *Mol Cell Biol* **20**, 3781-94 (2000).
63. Heibein, J. A. et al. Granzyme B-mediated cytochrome c release is regulated by the Bcl-2 family members bid and Bax. *J Exp Med* **192**, 1391-402 (2000).

6. References

64. Sutton, V. R. et al. Initiation of apoptosis by granzyme B requires direct cleavage of bid, but not direct granzyme B-mediated caspase activation. *J Exp Med* **192**, 1403-14 (2000).
65. Alimonti, J. B., Shi, L., Baijal, P. K. & Greenberg, A. H. Granzyme B induces BID-mediated cytochrome c release and mitochondrial permeability transition. *J Biol Chem* **276**, 6974-82 (2001).
66. Sharif-Askari, E. et al. Direct cleavage of the human DNA fragmentation factor-45 by granzyme B induces caspase-activated DNase release and DNA fragmentation. *Embo J* **20**, 3101-13 (2001).
67. Trapani, J. A. & Smyth, M. J. Functional significance of the perforin/granzyme cell death pathway. *Nat Rev Immunol* **2**, 735-47 (2002).
68. Shi, L. et al. Granzyme B (GraB) autonomously crosses the cell membrane and perforin initiates apoptosis and GraB nuclear localization. *J Exp Med* **185**, 855-66 (1997).
69. Trapani, J. A., Browne, K. A., Smyth, M. J. & Jans, D. A. Localization of granzyme B in the nucleus. A putative role in the mechanism of cytotoxic lymphocyte-mediated apoptosis. *J Biol Chem* **271**, 4127-33 (1996).
70. Pinkoski, M. J. et al. Entry and trafficking of granzyme B in target cells during granzyme B-perforin-mediated apoptosis. *Blood* **92**, 1044-54 (1998).
71. Froelich, C. J. et al. New paradigm for lymphocyte granule-mediated cytotoxicity. Target cells bind and internalize granzyme B, but an endosomolytic agent is necessary for cytosolic delivery and subsequent apoptosis. *J Biol Chem* **271**, 29073-9 (1996).

6. References

72. Metkar, S. S. et al. Cytotoxic cell granule-mediated apoptosis: perforin delivers granzyme B-serglycin complexes into target cells without plasma membrane pore formation. *Immunity* **16**, 417-28 (2002).
73. Motyka, B. et al. Mannose 6-phosphate/insulin-like growth factor II receptor is a death receptor for granzyme B during cytotoxic T cell-induced apoptosis. *Cell* **103**, 491-500 (2000).
74. Nalefski, E. A. & Falke, J. J. The C2 domain calcium-binding motif: structural and functional diversity. *Protein Sci* **5**, 2375-90 (1996).
75. Murray, D. & Honig, B. Electrostatic control of the membrane targeting of C2 domains. *Mol Cell* **9**, 145-54 (2002).
76. Esser, M. T., Haverstick, D. M., Fuller, C. L., Gullo, C. A. & Braciale, V. L. Ca²⁺ signaling modulates cytolytic T lymphocyte effector functions. *J Exp Med* **187**, 1057-67 (1998).
77. Sun, J. et al. A cytosolic granzyme B inhibitor related to the viral apoptotic regulator cytokine response modifier A is present in cytotoxic lymphocytes. *J Biol Chem* **271**, 27802-9 (1996).
78. Bird, C. H. et al. Nucleocytoplasmic distribution of the ovalbumin serpin PI-9 requires a nonconventional nuclear import pathway and the export factor Crm1. *Mol Cell Biol* **21**, 5396-407 (2001).
79. Kannan-Thulasiraman, P. & Shapiro, D. J. Modulators of inflammation use nuclear factor-kappa B and activator protein-1 sites to induce the caspase-1 and granzyme B inhibitor, proteinase inhibitor 9. *J Biol Chem* **277**, 41230-9 (2002).
80. Barrie, M. B., Stout, H. W., Abougergi, M. S., Miller, B. C. & Thiele, D. L. Antiviral cytokines induce hepatic expression of the granzyme B inhibitors,

6. References

- proteinase inhibitor 9 and serine proteinase inhibitor 6. *J Immunol* **172**, 6453-9 (2004).
81. Potempa, J., Korzus, E. & Travis, J. The serpin superfamily of proteinase inhibitors: structure, function, and regulation. *J Biol Chem* **269**, 15957-60 (1994).
82. Silverman, G. A. et al. The serpins are an expanding superfamily of structurally similar but functionally diverse proteins. Evolution, mechanism of inhibition, novel functions, and a revised nomenclature. *J Biol Chem* **276**, 33293-6 (2001).
83. Balaji, K. N., Schaschke, N., Machleidt, W., Catalfamo, M. & Henkart, P. A. Surface cathepsin B protects cytotoxic lymphocytes from self-destruction after degranulation. *J Exp Med* **196**, 493-503 (2002).
84. Dupuis, M., Schaerer, E., Krause, K. H. & Tschopp, J. The calcium-binding protein calreticulin is a major constituent of lytic granules in cytolytic T lymphocytes. *J Exp Med* **177**, 1-7 (1993).
85. Fraser, S. A., Karimi, R., Michalak, M. & Hudig, D. Perforin lytic activity is controlled by calreticulin. *J Immunol* **164**, 4150-5 (2000).
86. Samelson, L. E. Signal transduction mediated by the T cell antigen receptor: the role of adapter proteins. *Annu Rev Immunol* **20**, 371-94 (2002).
87. Clevers, H., Alarcon, B., Wileman, T. & Terhorst, C. The T cell receptor/CD3 complex: a dynamic protein ensemble. *Annu Rev Immunol* **6**, 629-62 (1988).
88. Osman, N., Turner, H., Lucas, S., Reif, K. & Cantrell, D. A. The protein interactions of the immunoglobulin receptor family tyrosine-based activation motifs present in the T cell receptor zeta subunits and the CD3 gamma, delta and epsilon chains. *Eur J Immunol* **26**, 1063-8 (1996).

6. References

89. de Aoz, I. et al. Tyrosine phosphorylation of the CD3-epsilon subunit of the T cell antigen receptor mediates enhanced association with phosphatidylinositol 3-kinase in Jurkat T cells. *J Biol Chem* **272**, 25310-8 (1997).
90. Guirado, M. et al. Phosphorylation of the N-terminal and C-terminal CD3-epsilon-ITAM tyrosines is differentially regulated in T cells. *Biochem Biophys Res Commun* **291**, 574-81 (2002).
91. Abraham, N., Miceli, M. C., Parnes, J. R. & Veillette, A. Enhancement of T-cell responsiveness by the lymphocyte-specific tyrosine protein kinase p56lck. *Nature* **350**, 62-6 (1991).
92. Straus, D. B. & Weiss, A. Genetic evidence for the involvement of the lck tyrosine kinase in signal transduction through the T cell antigen receptor. *Cell* **70**, 585-93 (1992).
93. Straus, D. B. & Weiss, A. The CD3 chains of the T cell antigen receptor associate with the ZAP-70 tyrosine kinase and are tyrosine phosphorylated after receptor stimulation. *J Exp Med* **178**, 1523-30 (1993).
94. Wange, R. L., Malek, S. N., Desiderio, S. & Samelson, L. E. Tandem SH2 domains of ZAP-70 bind to T cell antigen receptor zeta and CD3 epsilon from activated Jurkat T cells. *J Biol Chem* **268**, 19797-801 (1993).
95. Thome, M., Duplay, P., Guttinger, M. & Acuto, O. Syk and ZAP-70 mediate recruitment of p56lck/CD4 to the activated T cell receptor/CD3/zeta complex. *J Exp Med* **181**, 1997-2006 (1995).
96. Yokosuka, T. et al. Newly generated T cell receptor microclusters initiate and sustain T cell activation by recruitment of Zap70 and SLP-76. *Nat Immunol* **6**, 1253-62 (2005).

6. References

97. Zhang, W., Sloan-Lancaster, J., Kitchen, J., Tribble, R. P. & Samelson, L. E. LAT: the ZAP-70 tyrosine kinase substrate that links T cell receptor to cellular activation. *Cell* **92**, 83-92 (1998).
98. Griffith, C. E., Zhang, W. & Wange, R. L. ZAP-70-dependent and -independent activation of Erk in Jurkat T cells. Differences in signaling induced by H₂O₂ and Cd3 cross-linking. *J Biol Chem* **273**, 10771-6 (1998).
99. Shan, X. & Wange, R. L. Itk/Emt/Tsk activation in response to CD3 cross-linking in Jurkat T cells requires ZAP-70 and Lat and is independent of membrane recruitment. *J Biol Chem* **274**, 29323-30 (1999).
100. Herndon, T. M., Shan, X. C., Tsokos, G. C. & Wange, R. L. ZAP-70 and SLP-76 regulate protein kinase C- θ and NF- κ B activation in response to engagement of CD3 and CD28. *J Immunol* **166**, 5654-64 (2001).
101. Meinel, E. et al. Herpesvirus saimiri replaces ZAP-70 for CD3- and CD2-mediated T cell activation. *J Biol Chem* **276**, 36902-8 (2001).
102. Choudhuri, K. & van der Merwe, P. A. Molecular mechanisms involved in T cell receptor triggering. *Semin Immunol* **19**, 255-61 (2007).
103. Lee, K. H. et al. T cell receptor signaling precedes immunological synapse formation. *Science* **295**, 1539-42 (2002).
104. Alcover, A. & Alarcon, B. Internalization and intracellular fate of TCR-CD3 complexes. *Crit Rev Immunol* **20**, 325-46 (2000).
105. Liu, H., Rhodes, M., Wiest, D. L. & Vignali, D. A. On the dynamics of TCR:CD3 complex cell surface expression and downmodulation. *Immunity* **13**, 665-75 (2000).

6. References

106. Das, V. et al. Activation-induced polarized recycling targets T cell antigen receptors to the immunological synapse; involvement of SNARE complexes. *Immunity* **20**, 577-88 (2004).
107. Luton, F., Buferne, M., Davoust, J., Schmitt-Verhulst, A. M. & Boyer, C. Evidence for protein tyrosine kinase involvement in ligand-induced TCR/CD3 internalization and surface redistribution. *J Immunol* **153**, 63-72 (1994).
108. Mariathasan, S., Bachmann, M. F., Bouchard, D., Ohteki, T. & Ohashi, P. S. Degree of TCR internalization and Ca²⁺ flux correlates with thymocyte selection. *J Immunol* **161**, 6030-7 (1998).
109. Huang, J. F. et al. TCR-Mediated internalization of peptide-MHC complexes acquired by T cells. *Science* **286**, 952-4 (1999).
110. D'Oro, U. et al. Regulation of constitutive TCR internalization by the zeta-chain. *J Immunol* **169**, 6269-78 (2002).
111. Dustin, M. L. & Shaw, A. S. Costimulation: building an immunological synapse. *Science* **283**, 649-50 (1999).
112. Monks, C. R., Freiberg, B. A., Kupfer, H., Sciaky, N. & Kupfer, A. Three-dimensional segregation of supramolecular activation clusters in T cells. *Nature* **395**, 82-6 (1998).
113. Bunnell, S. C., Kapoor, V., Tribble, R. P., Zhang, W. & Samelson, L. E. Dynamic actin polymerization drives T cell receptor-induced spreading: a role for the signal transduction adaptor LAT. *Immunity* **14**, 315-29 (2001).
114. Tskvitaria-Fuller, I., Rozelle, A. L., Yin, H. L. & Wulfiging, C. Regulation of sustained actin dynamics by the TCR and costimulation as a mechanism of receptor localization. *J Immunol* **171**, 2287-95 (2003).

6. References

115. Kupfer, A. & Dennert, G. Reorientation of the microtubule-organizing center and the Golgi apparatus in cloned cytotoxic lymphocytes triggered by binding to lysable target cells. *J Immunol* **133**, 2762-6 (1984).
116. Grakoui, A. et al. The immunological synapse: a molecular machine controlling T cell activation. *Science* **285**, 221-7 (1999).
117. Billadeau, D. D., Nolz, J. C. & Gomez, T. S. Regulation of T-cell activation by the cytoskeleton. *Nat Rev Immunol* **7**, 131-43 (2007).
118. Cullinan, P., Sperling, A. I. & Burkhardt, J. K. The distal pole complex: a novel membrane domain distal to the immunological synapse. *Immunol Rev* **189**, 111-22 (2002).
119. Valitutti, S., Dessing, M., Aktories, K., Gallati, H. & Lanzavecchia, A. Sustained signaling leading to T cell activation results from prolonged T cell receptor occupancy. Role of T cell actin cytoskeleton. *J Exp Med* **181**, 577-84 (1995).
120. Krummel, M. F., Sjaastad, M. D., Wulfig, C. & Davis, M. M. Differential clustering of CD4 and CD3zeta during T cell recognition. *Science* **289**, 1349-52 (2000).
121. Caplan, S. & Baniyash, M. Searching for significance in TCR-cytoskeleton interactions. *Immunol Today* **21**, 223-8 (2000).
122. Rozdzial, M. M., Malissen, B. & Finkel, T. H. Tyrosine-phosphorylated T cell receptor zeta chain associates with the actin cytoskeleton upon activation of mature T lymphocytes. *Immunity* **3**, 623-33 (1995).
123. Morgan, M. M. et al. Superantigen-induced T cell:B cell conjugation is mediated by LFA-1 and requires signaling through Lck, but not ZAP-70. *J Immunol* **167**, 5708-18 (2001).

6. References

124. Labno, C. M. et al. Itk functions to control actin polymerization at the immune synapse through localized activation of Cdc42 and WASP. *Curr Biol* **13**, 1619-24 (2003).
125. Dombroski, D. et al. Kinase-independent functions for Itk in TCR-induced regulation of Vav and the actin cytoskeleton. *J Immunol* **174**, 1385-92 (2005).
126. Bubeck Wardenburg, J. et al. Regulation of PAK activation and the T cell cytoskeleton by the linker protein SLP-76. *Immunity* **9**, 607-16 (1998).
127. Zeng, R. et al. SLP-76 coordinates Nck-dependent Wiskott-Aldrich syndrome protein recruitment with Vav-1/Cdc42-dependent Wiskott-Aldrich syndrome protein activation at the T cell-APC contact site. *J Immunol* **171**, 1360-8 (2003).
128. Anton, I. M. et al. WIP deficiency reveals a differential role for WIP and the actin cytoskeleton in T and B cell activation. *Immunity* **16**, 193-204 (2002).
129. Turner, M. & Billadeau, D. D. VAV proteins as signal integrators for multi-subunit immune-recognition receptors. *Nat Rev Immunol* **2**, 476-86 (2002).
130. Badour, K. et al. The Wiskott-Aldrich syndrome protein acts downstream of CD2 and the CD2AP and PSTPIP1 adaptors to promote formation of the immunological synapse. *Immunity* **18**, 141-54 (2003).
131. Stowers, L., Yelon, D., Berg, L. J. & Chant, J. Regulation of the polarization of T cells toward antigen-presenting cells by Ras-related GTPase CDC42. *Proc Natl Acad Sci U S A* **92**, 5027-31 (1995).
132. Lowin-Kropf, B., Shapiro, V. S. & Weiss, A. Cytoskeletal polarization of T cells is regulated by an immunoreceptor tyrosine-based activation motif-dependent mechanism. *J Cell Biol* **140**, 861-71 (1998).

6. References

133. Ardouin, L. et al. Vav1 transduces TCR signals required for LFA-1 function and cell polarization at the immunological synapse. *Eur J Immunol* **33**, 790-7 (2003).
134. Kuhne, M. R. et al. Linker for activation of T cells, zeta-associated protein-70, and Src homology 2 domain-containing leukocyte protein-76 are required for TCR-induced microtubule-organizing center polarization. *J Immunol* **171**, 860-6 (2003).
135. Martin-Cofreces, N. B. et al. Role of Fyn in the rearrangement of tubulin cytoskeleton induced through TCR. *J Immunol* **176**, 4201-7 (2006).
136. Stinchcombe, J. C., Majorovits, E., Bossi, G., Fuller, S. & Griffiths, G. M. Centrosome polarization delivers secretory granules to the immunological synapse. *Nature* **443**, 462-5 (2006).
137. Becherer, U. & Rettig, J. Vesicle pools, docking, priming, and release. *Cell Tissue Res* **326**, 393-407 (2006).
138. Jahn, R. & Scheller, R. H. SNAREs--engines for membrane fusion. *Nat Rev Mol Cell Biol* **7**, 631-43 (2006).
139. Sudhof, T. C. & Rothman, J. E. Membrane fusion: grappling with SNARE and SM proteins. *Science* **323**, 474-7 (2009).
140. Ungar, D. & Hughson, F. M. SNARE protein structure and function. *Annu Rev Cell Dev Biol* **19**, 493-517 (2003).
141. Stow, J. L., Manderson, A. P. & Murray, R. Z. SNAREing immunity: the role of SNAREs in the immune system. *Nat Rev Immunol* **6**, 919-29 (2006).
142. Arneson, L. N. et al. Cutting edge: syntaxin 11 regulates lymphocyte-mediated secretion and cytotoxicity. *J Immunol* **179**, 3397-401 (2007).

6. References

143. Bryceson, Y. T. et al. Defective cytotoxic lymphocyte degranulation in syntaxin-11 deficient familial hemophagocytic lymphohistiocytosis 4 (FHL4) patients. *Blood* **110**, 1906-15 (2007).
144. zur Stadt, U. et al. Linkage of familial hemophagocytic lymphohistiocytosis (FHL) type-4 to chromosome 6q24 and identification of mutations in syntaxin 11. *Hum Mol Genet* **14**, 827-34 (2005).
145. Feldmann, J. et al. Munc13-4 is essential for cytolytic granules fusion and is mutated in a form of familial hemophagocytic lymphohistiocytosis (FHL3). *Cell* **115**, 461-73 (2003).
146. Menasche, G. et al. Mutations in RAB27A cause Griscelli syndrome associated with haemophagocytic syndrome. *Nat Genet* **25**, 173-6 (2000).
147. Fischer, A., Latour, S. & de Saint Basile, G. Genetic defects affecting lymphocyte cytotoxicity. *Curr Opin Immunol* **19**, 348-53 (2007).
148. Menasche, G., Feldmann, J., Fischer, A. & de Saint Basile, G. Primary hemophagocytic syndromes point to a direct link between lymphocyte cytotoxicity and homeostasis. *Immunol Rev* **203**, 165-79 (2005).
149. Latour, S. & Veillette, A. The SAP family of adaptors in immune regulation. *Semin Immunol* **16**, 409-19 (2004).
150. Nichols, K. E., Ma, C. S., Cannons, J. L., Schwartzberg, P. L. & Tangye, S. G. Molecular and cellular pathogenesis of X-linked lymphoproliferative disease. *Immunol Rev* **203**, 180-99 (2005).
151. Oh, J. et al. Positional cloning of a gene for Hermansky-Pudlak syndrome, a disorder of cytoplasmic organelles. *Nat Genet* **14**, 300-6 (1996).

6. References

152. Oh, J. et al. Mutation analysis of patients with Hermansky-Pudlak syndrome: a frameshift hot spot in the HPS gene and apparent locus heterogeneity. *Am J Hum Genet* **62**, 593-8 (1998).
153. Stinchcombe, J., Bossi, G. & Griffiths, G. M. Linking albinism and immunity: the secrets of secretory lysosomes. *Science* **305**, 55-9 (2004).
154. Clark, R. H. et al. Adaptor protein 3-dependent microtubule-mediated movement of lytic granules to the immunological synapse. *Nat Immunol* **4**, 1111-20 (2003).
155. Enders, A. et al. Lethal hemophagocytic lymphohistiocytosis in Hermansky-Pudlak syndrome type II. *Blood* **108**, 81-7 (2006).
156. Dell'Angelica, E. C., Shotelersuk, V., Aguilar, R. C., Gahl, W. A. & Bonifacino, J. S. Altered trafficking of lysosomal proteins in Hermansky-Pudlak syndrome due to mutations in the beta 3A subunit of the AP-3 adaptor. *Mol Cell* **3**, 11-21 (1999).
157. Ihrke, G., Kytala, A., Russell, M. R., Rous, B. A. & Luzio, J. P. Differential use of two AP-3-mediated pathways by lysosomal membrane proteins. *Traffic* **5**, 946-62 (2004).
158. Peden, A. A. et al. Localization of the AP-3 adaptor complex defines a novel endosomal exit site for lysosomal membrane proteins. *J Cell Biol* **164**, 1065-76 (2004).
159. Griscelli, C. et al. A syndrome associating partial albinism and immunodeficiency. *Am J Med* **65**, 691-702 (1978).
160. Klein, C. et al. Partial albinism with immunodeficiency (Griscelli syndrome). *J Pediatr* **125**, 886-95 (1994).

6. References

161. Wilson, S. M. et al. A mutation in Rab27a causes the vesicle transport defects observed in ashen mice. *Proc Natl Acad Sci U S A* **97**, 7933-8 (2000).
162. Dufourcq-Lagelouse, R. et al. Linkage of familial hemophagocytic lymphohistiocytosis to 10q21-22 and evidence for heterogeneity. *Am J Hum Genet* **64**, 172-9 (1999).
163. Augustin, I., Rosenmund, C., Sudhof, T. C. & Brose, N. Munc13-1 is essential for fusion competence of glutamatergic synaptic vesicles. *Nature* **400**, 457-61 (1999).
164. Prekeris, R., Klumperman, J. & Scheller, R. H. Syntaxin 11 is an atypical SNARE abundant in the immune system. *Eur J Cell Biol* **79**, 771-80 (2000).
165. Valdez, A. C., Cabaniols, J. P., Brown, M. J. & Roche, P. A. Syntaxin 11 is associated with SNAP-23 on late endosomes and the trans-Golgi network. *J Cell Sci* **112 (Pt 6)**, 845-54 (1999).
166. Risma, K. A., Frayer, R. W., Filipovich, A. H. & Sumegi, J. Aberrant maturation of mutant perforin underlies the clinical diversity of hemophagocytic lymphohistiocytosis. *J Clin Invest* **116**, 182-92 (2006).
167. Voskoboinik, I., Thia, M. C. & Trapani, J. A. A functional analysis of the putative polymorphisms A91V and N252S and 22 missense perforin mutations associated with familial hemophagocytic lymphohistiocytosis. *Blood* **105**, 4700-6 (2005).
168. Schwarz, E. C. et al. Calcium dependence of T cell proliferation following focal stimulation. *Eur J Immunol* **37**, 2723-33 (2007).
169. Quintana, A. et al. T cell activation requires mitochondrial translocation to the immunological synapse. *Proc Natl Acad Sci U S A* **104**, 14418-23 (2007).

6. References

170. Mantei, A. et al. siRNA stabilization prolongs gene knockdown in primary T lymphocytes. *Eur J Immunol* **38**, 2616-25 (2008).
171. Rozen, S. & Skaletsky, H. Primer3 on the WWW for general users and for biologist programmers. *Methods Mol Biol* **132**, 365-86 (2000).
172. Zur Stadt, U. et al. Mutation spectrum in children with primary hemophagocytic lymphohistiocytosis: molecular and functional analyses of PRF1, UNC13D, STX11, and RAB27A. *Hum Mutat* **27**, 62-8 (2006).
173. Sheff, D., Pelletier, L., O'Connell, C. B., Warren, G. & Mellman, I. Transferrin receptor recycling in the absence of perinuclear recycling endosomes. *J Cell Biol* **156**, 797-804 (2002).
174. van Dam, E. M. & Stoorvogel, W. Dynamin-dependent transferrin receptor recycling by endosome-derived clathrin-coated vesicles. *Mol Biol Cell* **13**, 169-82 (2002).
175. Ghosh, P. & Kornfeld, S. The GGA proteins: key players in protein sorting at the trans-Golgi network. *Eur J Cell Biol* **83**, 257-62 (2004).
176. Puri, S. & Linstedt, A. D. Capacity of the golgi apparatus for biogenesis from the endoplasmic reticulum. *Mol Biol Cell* **14**, 5011-8 (2003).
177. Hirst, J., Miller, S. E., Taylor, M. J., von Mollard, G. F. & Robinson, M. S. EpsinR is an adaptor for the SNARE protein Vti1b. *Mol Biol Cell* **15**, 5593-602 (2004).
178. Miller, S. E., Collins, B. M., McCoy, A. J., Robinson, M. S. & Owen, D. J. A SNARE-adaptor interaction is a new mode of cargo recognition in clathrin-coated vesicles. *Nature* **450**, 570-4 (2007).

6. References

179. Purbhoo, M. A., Irvine, D. J., Huppa, J. B. & Davis, M. M. T cell killing does not require the formation of a stable mature immunological synapse. *Nat Immunol* **5**, 524-30 (2004).
180. Dustin, M. L. T-cell activation through immunological synapses and kinapses. *Immunol Rev* **221**, 77-89 (2008).
181. Krummel, M. F. Immunological synapses: breaking up may be good to do. *Cell* **129**, 653-5 (2007).
182. Sims, T. N. et al. Opposing effects of PKC θ and WASp on symmetry breaking and relocation of the immunological synapse. *Cell* **129**, 773-85 (2007).
183. Kupfer, A. & Singer, S. J. The specific interaction of helper T cells and antigen-presenting B cells. IV. Membrane and cytoskeletal reorganizations in the bound T cell as a function of antigen dose. *J Exp Med* **170**, 1697-713 (1989).
184. Patino-Lopez, G. et al. Rab35 and its GAP EPI64C in T cells regulate receptor recycling and immunological synapse formation. *J Biol Chem* **283**, 18323-30 (2008).
185. Letourneur, F. & Klausner, R. D. A novel di-leucine motif and a tyrosine-based motif independently mediate lysosomal targeting and endocytosis of CD3 chains. *Cell* **69**, 1143-57 (1992).
186. Valitutti, S., Muller, S., Salio, M. & Lanzavecchia, A. Degradation of T cell receptor (TCR)-CD3-zeta complexes after antigenic stimulation. *J Exp Med* **185**, 1859-64 (1997).
187. de Brito, O. M. & Scorrano, L. Mitofusin 2 tethers endoplasmic reticulum to mitochondria. *Nature* **456**, 605-10 (2008).

6. References

188. Manderson, A. P., Kay, J. G., Hammond, L. A., Brown, D. L. & Stow, J. L. Subcompartments of the macrophage recycling endosome direct the differential secretion of IL-6 and TNFalpha. *J Cell Biol* **178**, 57-69 (2007).
189. Bright, N. A., Reaves, B. J., Mullock, B. M. & Luzio, J. P. Dense core lysosomes can fuse with late endosomes and are re-formed from the resultant hybrid organelles. *J Cell Sci* **110 (Pt 17)**, 2027-40 (1997).
190. Weisswange, I., Newsome, T. P., Schleich, S. & Way, M. The rate of N-WASP exchange limits the extent of ARP2/3-complex-dependent actin-based motility. *Nature* **458**, 87-91 (2009).
191. Menager, M. M. et al. Secretory cytotoxic granule maturation and exocytosis require the effector protein hMunc13-4. *Nat Immunol* **8**, 257-67 (2007).
192. Mascia, L. & Langosch, D. Evidence that late-endosomal SNARE multimerization complex is promoted by transmembrane segments. *Biochim Biophys Acta* **1768**, 457-66 (2007).
193. Kupfer, A., Dennert, G. & Singer, S. J. The reorientation of the Golgi apparatus and the microtubule-organizing center in the cytotoxic effector cell is a prerequisite in the lysis of bound target cells. *J Mol Cell Immunol* **2**, 37-49 (1985).
194. Makedonas, G. et al. Rapid up-regulation and granule-independent transport of perforin to the immunological synapse define a novel mechanism of antigen-specific CD8+ T cell cytotoxic activity. *J Immunol* **182**, 5560-9 (2009).
195. Peters, P. J. et al. Molecules relevant for T cell-target cell interaction are present in cytolytic granules of human T lymphocytes. *Eur J Immunol* **19**, 1469-75 (1989).

7. Publications

- Bin Qu^{*}, Varsha Pattu^{*}, Christian Junker, Eva C. Schwarz, Misty Marshall, Ute Becherer, Ulf Matti, Heiko Rieger, Jens Rettig[#], Markus Hoth[#]. Effective CTL function requires Vti1b-dependent interaction between lytic granules and endocytosed TCR compartments. (*submitted*)
- Bin Qu^{*}, Varsha Pattu^{*}, Eva C. Schwarz, Shruthi Bhat, Jens Rettig[#], Markus Hoth[#]. Characterization of SNARE proteins in cytotoxic T lymphocytes. (*in preparation*)
- Varsha Pattu^{*}, Bin Qu^{*}, Misty Marshall, Eva C. Schwarz, Shruthi Bhat, Markus Hoth[#], Jens Rettig[#]. Syntaxin 7 is required for the release of lytic granules in cytotoxic T lymphocytes. (*in preparation*)
- Jiuhong Kang^{*}, Yufeng Shi^{*}, Bin Xiang^{*}, Bin Qu, Wenjuan Su, Min Zhu, Min Zhang, Guobin Bao, Feifei Wang, Xiaoqing Zhang, Rongxi Yang, Fengjuan Fan, Xiaoqing Chen, Gang Pei[#] and Lan Ma[#]. A nuclear function of beta-arrestin1 in GPCR signaling: regulation of histone acetylation and gene transcription. *Cell* 123: 833-847 (2005).
- Hua Gao^{*}, Yue Sun^{*}, Yalan Wu, Bing Luan, Yaya Wang, Bin Qu and Gang Pei. Identification of beta-arrestin2 as a G protein-coupled receptor-stimulated regulator of NF-kappaB pathways. *Mol Cell*. 14(3): 303-17 (2004)
- Gufa Lin, Xin Geng, Ying Chen, Bin Qu, Fubin Wang, Ruiying Hu, Xiaoyan Ding. T-box binding site mediates the dorsal activation of myf-5 in *Xenopus* gastrula embryos. *Dev Dyn*. 226(1): 51-8 (2002).

* These authors contributed equally to this work

These authors contributed equally to this work

8. Acknowledgements

My deepest gratitude goes first and foremost to Prof. Dr. Markus Hoth, my supervisor, for his constant encouragement and guidance. He has walked me through all the stages of my work. Without his consistent support, patience and understanding, this thesis would not have reached its present form. I would like to specially mention how much I admire the niceness in him. I am happy that I got such a wonderful PhD supervisor from whom I learned not only science but also about the qualities of a role model.

I would also like to sincerely thank and appreciate Prof. Dr. Jens Rettig for his valuable suggestions and his support for my work. I am also greatly indebted Dr. Eva C. Schwarz, who introduced to me all techniques with great patience in the beginning and helped me a lot throughout my work. I also thank Varsha Pattu, with whom I had a pleasant cooperation during my PhD. She offered great help for my work and accompanied me through my ups and downs.

For the generous assistance in my research, I would like to acknowledge our entire group, with special thanks to Christian Junker, Shruthi Bhat, Meledie-Jo Wolfs, Shruthi Bhat, Bettina Strauß, Anja Ludes, Claudia Kilter and our secretary Regine Kaleja and the former secretary Ute Legler. My gratitude also goes to Prof. Rettig's group, especially to Dr. Misty Marshall, Dr. Claudia Schirra, Dr. Ulf Matti and Dr. Ute Becherer.

I am also grateful to Prof. Dr. Heiko Rieger for formulating the compartment model and to Prof. Dr. Peter Lipp for use of confocal microscope. My thanks also to the graduate school of *Calcium Signalling and cellular nandomains* for the generous financial support and for the helpful scientific training courses arranged and coordinated by Prof. Dr. Dieter Bruns and Judith Wolf.

And finally, I cannot thank my beloved family, especially my husband Wei, enough for their deep love and constant belief in me through all these years. I also owe my sincere gratitude to my friends who gave me their time in helping me work out my problems during my difficult times.

9. Curriculum Vitae

PERSONAL INFORMATION

Name: Bin Qu
Date of Birth: 27/03/1980
Gender: Female
Nationality: Chinese
Tel: +49 6841 16-26458
Fax: +49 6841 16-26060
E-mail: bin.qu@uks.eu

EDUCATION

2006-present **Ph.D candidate** in the International PhD-Program '*Calcium-Signaling and Cellular Nanodomains*', at Saarland University, Homburg/Saar, Germany
Supervisor: Prof. Dr. Markus Hoth

2002-2005 **Master of Science**
The Institute of Biochemistry and Cell Biology, Shanghai Institutes for Biological Sciences (SIBS), Chinese Academy of Sciences (CAS)
Supervisor: Prof. Dr. Gang Pei

1997-2001 **Bachelor of Science**
Biological Science, University of Science and Technology of China